This document is currently under revision by the European Commission (EC) and has not yet been validated or approved by the EC. The content provided herein is subject to change, and the information presented may not represent the final position or official stance of the EC.

This document is being shared for informational purposes only and is not to be considered an official or authoritative source of information from the European Commission. Any decisions, actions, or interpretations based on the content of this document should be taken with caution, as the content may be subject to modification or revision by the EC.

The EC accepts no liability for any inaccuracies, errors, or omissions in this document, and any reliance on its content is at the user's own risk. It is recommended to verify the information provided in this document with official EC publications or communications before making any decisions or drawing any conclusions based on its content.

Please note that the content in this document may be confidential or sensitive in nature and should be treated as such. Unauthorized dissemination, distribution, or use of this document is strictly prohibited.

By accessing and reviewing this document, you acknowledge and accept the terms of this disclaimer.

BL2F

Transforming Black Liquor to Biofuel

Research and Innovation Action
H2020-LC-SC3-2019-NZE-RES-CC

D1.2 - Report on HTL batch experiments

WP1 - Task 1.2

30th September 2022

Lead Beneficiary: KIT

Author(s): Maximilian Wörner (KIT), Ursel Hornung (KIT)

Reviewer(s): David Baudouin (PSI), Jukka Konttinen (TAU)

@BL2F_EU **www.bl2f.eu** **BL2F_EU**

Disclaimer

The content of this deliverable reflects only the author's view. The European Commission is not responsible for any use that may be made of the information it contains.

This project has received funding from the European Union's Horizon 2020 research and innovation programme under the Grant Agreement n°884111.

Document Information

Grant agreement	884111
Project title	Black Liquor to Fuel by Efficient Hydrothermal Application integrated to Pulp Mill
Project acronym	BL2F
Project coordinator	Prof. Dr. Tero Joronen
Project duration	1st April 2020 – 30th September 2023 (42 Months)
Related work package	WP 1 – HTL-oil production
Related task(s)	Task 1.2 – HTL batch experiments
Lead organisation	KIT
Contributing partner(s)	KIT, PSI
Due date	30th September 2022
Submission date	30th September
Dissemination level	Public

History

Date	Version	Submitted by	Reviewed by	Comments
	N°X			

Table of contents

List of figures

List of tables

Abbreviations and acronyms

Acronym	Description
WP	Work Package
BL	Black Liquor
ML	Model black liquor
HTL	Hydrothermal Liquefaction
KIT	Karlsruhe Institute of Technology
PSI	Paul-Scherrer Institute
w_{tr}	Dry mass content of BL
$w_{ash,815\,°C}$	Ash content of BL
$w_{tr,waf}$	Dried, water and ash free mass content of BL (=organics)
ρ_{BL}	Density BL
φ_i	Volume fraction of component *i*
K_i	Distribution coefficient for component *i* for liquid-liquid extraction with ethyl acetate
C	Carbon
H	Hydrogen
N	Nitrogen
S	Sulfur
O	Oxygen
Na	Sodium
K	Potassium
EA	Elemental analysis
ICP-OES	Inductively coupled plasma – optical emission spectrometry
GC	Gas chromatograph/chromatography

TCD	Temperature conductivity detector
FID	Flame ionization detector
MS	Mass spectroscopy
CO	Carbon monoxide
CO_2	Carbon dioxide
TOC	Total organic carbon
TC	Total carbon
TIC	Total inorganic carbon
NIST	National Institute of Standards and Technology
ISTD	Internal standard
DMSO	Dimethyl sulfoxide
SEC	Size exclusion chromatography
HPLC	High-performance liquid chromatography
IC	Ion chromatography
H_2S	Hydrogen sulfide
DMS	Dimethyl sulfide
DMDS	Dimethyl disulfide
DMTS	Dimethyl trisulfide
SCD	Sulfur chemiluminescence detector

Executive Summary

[The executive summary should place the deliverable within the overall project context, provide an overview of the key objectives, methods of development and results of the deliverable.]

Keywords

Black liquor, Fuel, Aviation, Shipping, Hydrothermal liquefaction, Model substances, Sulfur, Product analysis, dimethyl sulphide, biocrude, aromatic compound

1 Introduction

The BL2F project aims for developing novel technology for converting black liquor (BL) to fuel. As in any conversion process, knowing the quality of the feedstock is in key role. This report describes the results of characterization of BL. BL is a side stream of pulping of wood. The two main sources of pulp are soft wood (mainly spruce and pine) and hard wood (eucalyptus and birch). The selected primary feedstock in the BL2F project is BL from Kraft pulping of Eucalyptus. This report and the BL2F project do not handle BL from other feedstock, such as straw. The HTL of black liquor has gained increasing interest in the scientific community. A review of the BL and BL driven lignin is made in the BL2F project by Lappalainen et al. [1].

In Task 1.2 of the project, batch experiment studies of the hydrothermal liquefaction of black liquor are done at Karlsruhe Institute of Technology (KIT). The aim of the task is to go more in detail on the depolymerisation process of the lignin during the HTL. The influence of temperature and holding time is investigated as well as the influence of the sulfide salts coming from the cooking process (part of the Kraft process in the pulping industry). This deliverable shows the procedure of the experiments, the following analysis steps and discusses the results. The deliverable is divided in two parts. The first one is about the experiments with the real black liquor as feedstock, the second one is about experiments with model black liquors to investigate the behaviour of the sulfur and the sulfide salts.

2 HTL of real black liquor

2.1 Materials and methods

2.1.1 Feedstock

We used the black liquor from the pulp mill of our project partner, The Navigator Company in Portugal. The BL is used in its pristine form. It is a black almost homogeneous liquid (see **Figure 1**). The typical composition as well as the properties of the black liquor are given in Deliverable 1.1 (Feedstock Characterization). The important values for this deliverable are listed in the following tables. The feedstock was always stored in a refrigerator at 5 °C, which slows down possible oxidation processes. We did not freeze it, since mechanical destruction of the lignin molecules are possible during the freezing process.

Figure 1: pristine black liquor used in the experiments

w_{tr}	$w_{ash,815\,°C}$	$w_{tr,waf}$	ρ_{BL}	pH
14,5 wt. %	6,5 wt. %	8,4 wt. %	1,0725 kg*l^{-1}	> 12,5

Table 1: Properties of the used BL

Element symbol	Mass fraction in dry mass / wt. %
C (EA)	34
H (EA)	3,4
N (EA)	< 0,1
S (EA)	4,7
O (Diff.)	38,8
Na (ICP)	17,7
K (ICP)	1,3

Table 2: Elemental analysis and ICP results for dry mass from BL; oxygen calculated by difference

2.1.2 Experimental procedure

All the batch experiments were carried out in micro autoclaves crafted at the institute's own workshop. The autoclaves are made of stainless steel 1.4571 (316Ti) and have a volume V = 25 mL (see **Figure 2**). To close and open the micro autoclaves we used a special station, which is also connected to a gas trap, where we can take gas samples (see **Figure 3**).

Figure 2: Micro autoclaves used in the batch experiments

Figure 3: Micro autoclave station in the lab: a(container for the autoclaves; b) manometer to measure the pressure inside the system; c) septum for gas sample

The first step of the experimental procedure is to fill the black liquor into the micro autoclaves. The reactors should be weighed before and after the filling to get the exact weight of the used feedstock. The volume of the black liquor depends on the reaction temperature T_R since the temperature is correlating with the pressure. To maintain the pressure around 200 – 250 bar, we have to change the volumes for different temperature ranges. The respective volumes of black liquor at the different reaction temperatures are listed in the following **Table 4**.

T_R	250 – 275 °C	300 – 350 °C	375 °C	400 °C
V_{BL}	17,5 mL	15 mL	12,5 mL	5 mL

Table 3: Volumes of BL V_{BL} in micro autoclave at different reaction temperatures T_R

After the filling step, the autoclaves are placed inside the autoclave station, where they are purged with nitrogen to create an inert atmosphere. A pressure of approximately 10 bar is set and afterwards the reactor is tightly sealed. The pressure inside the autoclave helps to seal the reactor. To ensure that the preparation has worked, the autoclave is weighed again. The reaction process itself is done in a sand bath, where the reaction temperature T_R is set. The final temperature inside the reactor is reached after a heating time t_H = 10 min. This goes for every reaction temperature inside the investigated range. It was tested beforehand with a modified autoclave connected to a temperature sensor. In the further course, we will discuss the holding time t_R, which represents the time after t_H. Experiments were performed at different reaction conditions from 250 – 400 °C with t_R = 20 min and from 0 – 30 min with T_R = 375 °C. All of them were done at least in triplicates, and the resulting values show their average and standard deviation (error bars in figures). After the reaction process in the sand bath, the autoclaves are cooled down in a water bath to stop the ongoing reactions as fast as possible. To open the reactors, they are again placed in the micro autoclave station. All the lines connected to the gas trap are purged with nitrogen. Afterwards the reactor is ready to open. The gas is fed into the gas trap and can be extracted using a gas-tight syringe. Different pressures during the HTL process were not investigated. The influence of the pressure is not that big compared to temperature or holding time in parameter areas not directly around the critical point, where the phases and the properties are changing drastically [2]. Since adjusting the process conditions to an exact pressure is not so easy with our system, we decided not to do experiments with different pressures.

2.1.3 Analytical methods

The gas sample is injected into a GC 6890 Hewlett Packard gas chromatograph loaded with a thermal conductivity detector and a flame ionization detector (GC-TCD/FID). It is equipped with a Molsieve 5 A and a column Hayesep Q (both Restek).

To calculate the content of carbon in the gas phase, the volume fractions φ_i of CO, CO_2 and alkanes up to iso-butane as well as the olefins ethene and propene are measured. Since air content in the sample is unavoidable, the volume fraction must be corrected.

$$\varphi_{i,corr} = \frac{100 * \varphi_i}{100 - \varphi_{O_2} - (\varphi_{O_2} * \frac{78}{22})} \quad (1)$$

φ_{O_2} describes the measured volume fraction of oxygen in the sample. The ratio 78/22 stands for the N_2/O_2 ratio in the surrounding air. The second value which has to be corrected is the pressure p displayed on the manometer after opening the autoclave. Since it shows the

pressure for the whole system and not only for the pressure inside the micro autoclave, it is necessary to use previously determined correlation. For this, autoclaves were filled with different pressures and opened afterwards.

$$p_{corr} = \frac{p}{0.082} \quad (2)$$

To determine the amount of the individual gases n_i in the gas phase, the ideal gas law is used.

$$n_i = \frac{p_{corr} * V * \frac{\varphi_{i,corr}}{100}}{R * T_{room}} \quad (3)$$

The volume V describes the free volume of the micro autoclaves. The room temperature was always around $T_{room} \approx 296{,}15$ K. We set this value as a fixed constant. The universal gas constant is represented by $R = 8{,}314$ J/(mol*K). The last step for calculating the total detectable mass of carbon in the gas $m_{C,gas}$ is summation of the individual carbon masses of the detected gases. For molecules with multiple carbon atoms, the number of these is taken into account. With the number of carbon atoms in the molecule v_i and M_C as the molecular weight of carbon, the equation is given by

$$m_{c,g} = \left(\sum n_i * v_i\right) * M_C \quad (4)$$

After the gas sample analysis, the reactor is fully opened. A subsequently vacuum filtration is done for separation of the solid from the liquid. We used a nylon filter (diameter: 0,45 µm, Whatman) for the filtration. The residue in the reactor was declared as loss. Due to the low mass loss (see carbon mass balance later), we decided not to wash the residue from the reactor with a solvent. The solid residue is dried at 105 °C to evaporate the remaining water. Afterwards the solid sample is pulverized with a mortar and analyzed by elemental analysis (EA) and inductively coupled plasma - optical emission spectrometry (ICP-OES) to identify both the carbon content and possible precipitated salts (sodium, potassium). The filtrate represents the liquid product phase. We analyzed the TOC/TIC/TC content of an aliquot of the liquid sample using a Dimatoc 2100 (Dimatec Analysentechnik GmbH) for the completion of the carbon mass balance. The sample is diluted with ultrapure water (1:100). The instrument determines the total carbon (TC) and the inorganic carbon (TIC) in the sample. The organic carbon content (TOC) is then determined by difference.

A second aliquot is used to determine and quantify aromatic monomers with gas chromatographs (GC). To qualify unknown components, Agilent's GC 6890N equipped with a non-polar capillary column (Rfxi-5Sil, Restek) and an Agilent 5973 MSD mass spectrometry detector is used (GC-MS). The underlying database originates from the National Institute of Standards and Technology (NIST). The quantification of the most important aromatic monomer compounds was done with an Agilent GC 7820A with a FID. The column inside the GC-FID is the same we use in the GC-MS setup. The procedure for sample preparation is based on the method used by Forchheim et al. [3]. The sample has to be placed in the correct matrix first to obtain the best possible results later. At first, the sample must be acidified to a pH around 3-4. We use concentrated hydrochloric acid in this step (20 wt. %, approx. 6M). The acidified liquid phase in then filtered again with a syringe filter (pore size 0.22 µm) to remove the

precipitated components due to acidification. Afterwards 1,3 mL of the filtered sample is mixed with 0,52 mL of a prepared extractant in an Eppendorf tube. The used mixture contains mainly ethyl acetate, but also an internal standard (ISTD), pentadecane, which is needed later for quantification. The concentration of pentadecane is around 700 mg/L ethyl acetate. After mixing the sample and the extractant the tube is shaken for one minute and rested for a minimum of one hour. After the resting time is over, a clear phase separation is visible, in which the organic phase is the upper one. An aliquot of the organic phase is diluted in ethyl acetate (1:3 dilution) to get into the calibration range of the GC-FID. A total of ten different aromatic compounds can be quantified with our GC setup. For each of them a distribution coefficient K_i for the used extraction procedure was determined. The following table (see **Table 5**) list the components and the respective coefficient.

Component name	Distribution coefficient K_i
Phenol	0,95
Guaiacol	0,92
Catechol	0,82
3-Methoxycatechol	0,7
3-Methylcatechol	0,83
4-Methylcatechol	0,7
Syringol	0,75
4-Ethylcatechol	0,87
Syringaldehyd	0,67
Acetosyringon	0,65

Table 4: Distribution coefficient K_i for all quantified compounds with GC-FID in an ethyl acetate – water mixture

Together with the dilution factor *a*, the extraction volume factor *b*, the ISTD factor *c* and the raw data $\beta_{i,raw}$ of the GC-FID analysis following equation is given to determine the mass concentration of the compounds in the original samples.

$$\beta_i = \frac{\beta_{i,raw} * a * b * c}{K_i} \quad (5)$$

The dilution factor *a* describes the overall dilution of the original sample, the extraction volume factor *b* takes the ratio between the volume of the sample and the extractant into account and the ISTD factor *c* considers the ratio between the concentration of ISTD in the analyzed sample and the original ISTD concentration in the extractant.

To calculate the yields of the species $Y_{i,BM}$ to increase the comparability between processes, we need the mass of the feedstock m_{feed} in the reactor before processing and the mass of the collected liquid product phase $m_{liq,prod}$ as well as $m_{tr,waf}$ and m_{total}.

$$Y_{i,BM} = \frac{\frac{\beta_i}{\rho} * m_{liq,prod}}{\frac{m_{tr,waf}}{m_{total}} * m_{feed}} \quad (6)$$

In the next step, the average molecular weight of the biocrude is determined. For this step all the three samples of the same experiments were mixed together. Otherwise, we would not have enough sample for the next analysis steps. A standard deviation was not calculated for these results. The procedure is almost the same as for the sample preparation of the GC analysis. The difference is that the used volume of extracting agent is the same as the sample and it is evaporated to get only the organic matter from the liquid sample. A spatula tip of this is then dissolved in 2 - 3 mL dimethyl sulfoxide (DMSO) and analyzed by size exclusion chromatography (SEC). We choose DMSO as the eluent as well as the solvent, because it has the best ability to dissolve Lignin and its depolymerization products. Both of them have polar as well as unipolar groups. The best way to dissolve most of it without any functionalization step before is to use a solvent which can handle both, which is DMSO [4]. From the chromatograms obtained, the average molecular weight within the calibration limit can be determined. During the analysis, this was between 250 and 10000 g/mol. We use a Hitachi LaChrom diode array detector DAD L-2455 with a Viscotek A2500 column. The detector delivers an UV signal as a result. Quantitative analysis of a concentration in a specific weight interval is not possible due to lack of standards which have similar structures as lignin. Especially the mixture of nonpolar and polar parts are a problem.

The aqueous phase, which is produced during the extraction step to get the biocrude, is analyzed via high-perfomance liquid chromatography (HPLC) (Merck Hitachi Primade, DAD and detector. The used column (Aminex HPX 87H, Biorad) and the method is design for organic acids and alcohols. We are able to quantify formic acid, acetic acid, glycolic acid, lactic acid as well as methanol and ethanol.

2.2 Results and discussion

The results of the batch experiments with the pristine black liquor are presented in the following chapters. First, the carbon mass balance is highlighted. In the second part the production of aromatic monomers is covered. Last, the results of the GPC analysis are shown.

In general, the HTL products looked all similar. We got always three product phases. The solid one is a black powder. The liquid product only have one phase. The colour is brown varying

from dark to bright. At higher temperatures and longer holding times, the liquid becomes clearer and slightly reddish. As a third phase, we collected the gas in the gas trap.

2.2.1 Carbon mass balance

In **Figure 4** the carbon mass balance for the series of different reaction temperatures T_R with a holding time of t_R = 20 min is shown. The carbon content is divided into proportions in four different phases. These are the proportion in the solid, the inorganic and the organic proportion in the liquid phase, and the carbon content in the gas phase. In addition, there is a further category, the carbon deficit in the mass balance. Across all experimental points, 75 – 90 wt. % of carbon could be found in the product phases. The residue in the reactor as well as a possible loss of volatile and gaseous materials can explain the deficit of carbon. The carbon content in the gaseous phase generally does not have a large fraction. While the proportion is clearly visible at the higher temperatures from T_R = 375 °C, hardly any carbon is found in the gas phase at low temperatures. The largest proportion of carbon is found in carbon dioxide. The mass fraction of the overall gas is between 50 – 70 wt. %, the carbon mass content is between 30 – 60 wt. % of all carbon in the detected gas compounds. The CO_2 is formed by the decarboxylation reaction, which is one of the main reactions in the HTL of lignin. In addition, detectable carbon-containing gases are short-chain hydrocarbons, including both those with single and double bonds. The slight increase in inorganic carbon above temperature T_R = 300 °C is probably related to increased CO_2 formation. Dissolved CO_2 reacts in aqueous solution to form the carbonate. The two phases with the highest proportion of carbon are the organic carbon in the liquid phase and that bound in the solid phase. It can be clearly seen that the organic fraction decreases rapidly with increasing temperature. In parallel, the fraction allocated to the solid increases. At a reaction temperature T_R = 400 °C, almost half of the original total carbon is in the solid. This effect is negative with regard to a possible biocrude extraction, since fewer organic carbon compounds are present in the liquid phase. A possible explanation for the results arises when considering the batch process. While the experiments are easy to handle, they bring the disadvantages of a batch experiment compared to a continuous experiment. We assume that despite a near- or supercritical condition, mixing is not optimal. This problem can lead to increased incidence of crosslinking reactions between the aromatics and reactants formed, which would lead to an enhanced carbonization process occurs. This effect seems to accelerate especially at higher temperatures. In addition, the aromatic lignin structure also contributes to the fact that an increased degree of carbonization occurs. Aromatics tend to enter into char forming reactions more readily [5]. Analysis of the solid also confirms the accumulation of carbon in the solid (see **Table 5**). Another aspect of the carbon balance is the high organic content at T_R = 250 °C. The reason for this is probably the depolymerization of the lignin, which has not yet progressed far enough.

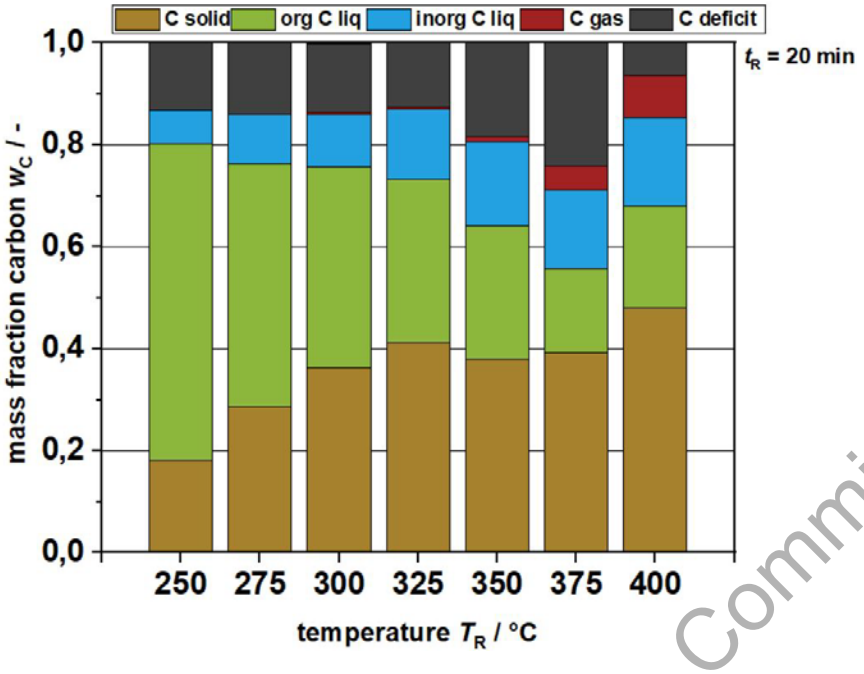

Figure 4: Carbon mass balance; T_R = 250 – 400 °C; t_R = 20 min; inorganic to organic carbon ratio in feedstock 1:24

	Mass fraction in dry mass / wt. %						
T_R	**250**	**275**	**300**	**325**	**350**	**375**	**400**
C (EA)	53	54,2	59	66,5	72,6	77,8	79,2
H (EA)	4,8	4,1	3,9	4,4	5,1	5,3	5,1
N (EA)	0,1	0,2	0,2	0,2	0,2	0,2	0,2
S (EA)	2	2,2	1,0	1,5	1,5	1,3	1,1
O (Diff.)	32,22	31,4	27,9	22,3	17,5	13,8	12
Na (ICP)	7,3	7,3	6,5	4,7	2,9	1,5	2,2
K (ICP)	0,6	0,6	0,5	< 0,5	< 0,5	< 0,5	< 0,5

Table 5: elemental analysis and ICP analysis of solid phase after HTL; oxygen calculate by difference, T_R variation

In addition to the carbon balance at different reaction temperatures T_R, we have also evaluated it for different holding times t_R = 0 - 30 min at a constant temperature T_R = 375 °C (see **Figure 5**). At first glance, it can be seen that the influence of the holding time is significantly smaller than that of the temperature. This can be explained by the fact that around the critical point the properties of water change drastically. Since an approach or removal from this point

does not occur with the holding time, the influence is somewhat smaller in this respect. Nevertheless, it can be seen from the balance that the organic carbon content in the liquid phase can be doubled at a holding time of t_R = 5 min or less compared to the experiment at t_R = 20 min. The higher losses at the constant reaction temperature T_R = 375 °C are due to a very sticky solid mass in the reactor. In **Table 6** the results of the solid phase analysis for the holding time variation are listed. In comparison to the solids from the temperature variation, there is only a little difference between the lowest and the highest holding time regarding the carbon content. Since there are variations in the overall solid mass the effect of increasing carbon content in the solid is negligible in the carbon mass balance. Another interesting observation on the mass fractions in the solid is the visible decarboxylation process. The oxygen content is reducing with higher temperatures and higher holding times. Together with the higher production of CO_2, which is the main reason for the increase of gaseous carbon in the mass balance, it is a clear sign for decarboxylation reactions. The comparison between the two tables containing the mass fractions in the solid phase shows also that sodium content is reducing with higher temperature and is stable with increasing holding times.

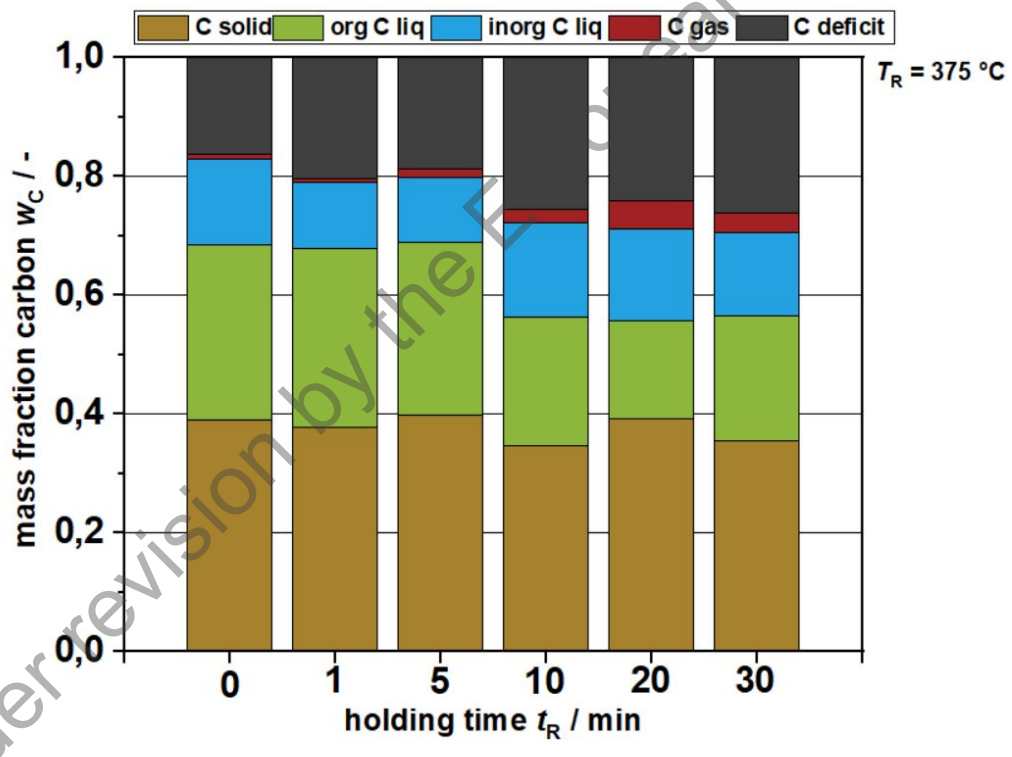

Figure 5: Carbon mass balance; t_R = 0 – 30 °C; T_R = 375 °C; inorganic to organic carbon ratio in feedstock 1:24

	Mass fraction in dry mass / wt. %					
t_R	**0**	**1**	**5**	**10**	**20**	**30**
C (EA)	67,9	72,8	73,8	76,6	77,8	79,3
H (EA)	4,6	5,3	5,3	5,6	5,3	5,5
N (EA)	0,2	0,1	0,1	0,1	0,2	0,1
S (EA)	1,3	1	1,3	1,1	1,3	1,1
O (Diff.)	25,8	20,2	19	16,2	13,8	13,7
Na (ICP)	x	0,5	0,5	0,4	1,5	0,3
K (ICP)	x	< 0,5	< 0,5	< 0,5	< 0,5	< 0,5

Table 6: elemental analysis and ICP analysis of solid phase after HTL; oxygen calculate by difference, t_R variation

2.2.2 Monomer compounds in the product

The next section of the product analysis deals with the monomers in the liquid product phase. In order to understand the HTL process, these are important indicators to better understand reaction steps. The focus here is primarily on aromatics, as these are the main products. We were able to qualify some of the main components by GC-MS and then quantify them by GC-FID. For the quantification, we restricted ourselves to the substances that left clear peaks in the chromatogram and were clearly identifiable (see **Table 4**). The aromatic compounds found correspond to the typical depolymerization products of lignin [6, 7]. This indicates that hydrothermal liquefaction also works when black liquor is used directly. Also visible in the chromatogram were some degradation products of hemicellulose, such as various carboxylic acids. These will not be discussed in detail here, as the focus of the work is on the depolymerization of the lignin molecule and the associated formation of the aromatics. **Figure 6** shows the yields of various aromatic compounds at different reaction temperatures T_R. It is clearly visible that catechol and its derivatives are the main products in the samples studied. While 3-methoxycatechol (blue) still has the highest yield of all aromatics at T_R = 250 °C, the molecule disappears very quickly at higher temperatures. Instead, other catechols are formed, primarily catechol (green) itself and 4-methylcatechol (pink). Interestingly, only small amounts of phenol (red) were quantified. Phenol has been classified more often as a major product in various papers on the HTL of lignin. Likewise, phenol derivatives such as cresols or xylenols were qualitatively detectable. Aromatics with functional groups like methoxy or carboxyl groups are hardly present at T_R = 300 °C while catechol with two hydroxy groups reaches maximum yield at this point. In addition, products with methyl compounds also increase. With further increasing reaction temperatures, all further yields also

decrease. At T_R = 400 °C, hardly any aromatic compounds which are detectable with the used GC methods are present. This observation fits to the observation of the carbon balance. The decrease in organic carbon can also be seen there as already described. The monoaromatics are decreasing even more than the overall organic carbon. These leads to the question what kind of other organic compounds are in the liquid product phase.

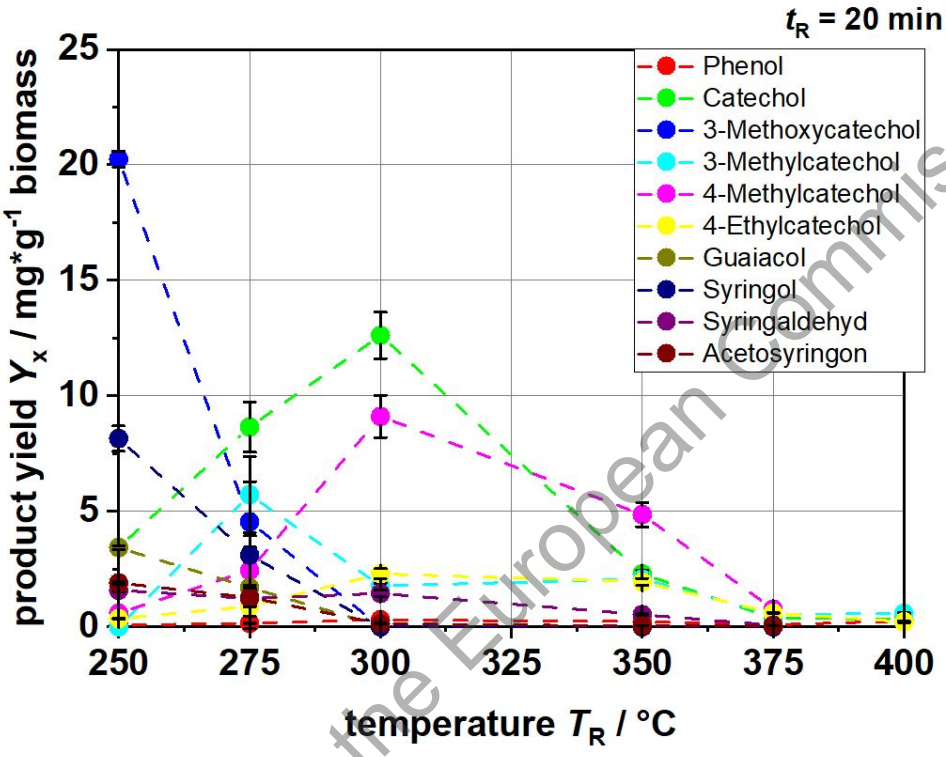

Figure 6: Product yields of aromatic compounds after HTL of black liquor; T_R = 250 – 400 °C; t_R = 20 min

As in the case of the mass balance, we also investigated the influence of the holding time t_R for the monomer yields. The results are shown in **Figure 7**. The experiment at a holding time of t_R = 0 min could not be evaluated due to technical problems. In general, the same substances were found as in the experiments with different reaction temperatures. Since the higher temperatures around T_R = 375 °C are more interesting for the project, we decided to perform the holding time variation at this temperature. At first, it is clearly visible, that we are able to significantly increase the yields of individual monomers with lower holding times. The same is true for organic carbon in general, see the results of the mass balances. The increase in yield mainly concerns catechols and their derivatives. In this case, especially the derivatives with alkyl groups are significantly increased. One reason for this may be the increased occurrence of methyl radicals at higher temperatures, which can react with the aromatic ring [8]. Overall, it

can be said that lower holding times are better for overall organic yields. It is true for the overall organic carbon as well as for the monoaromatic compounds.

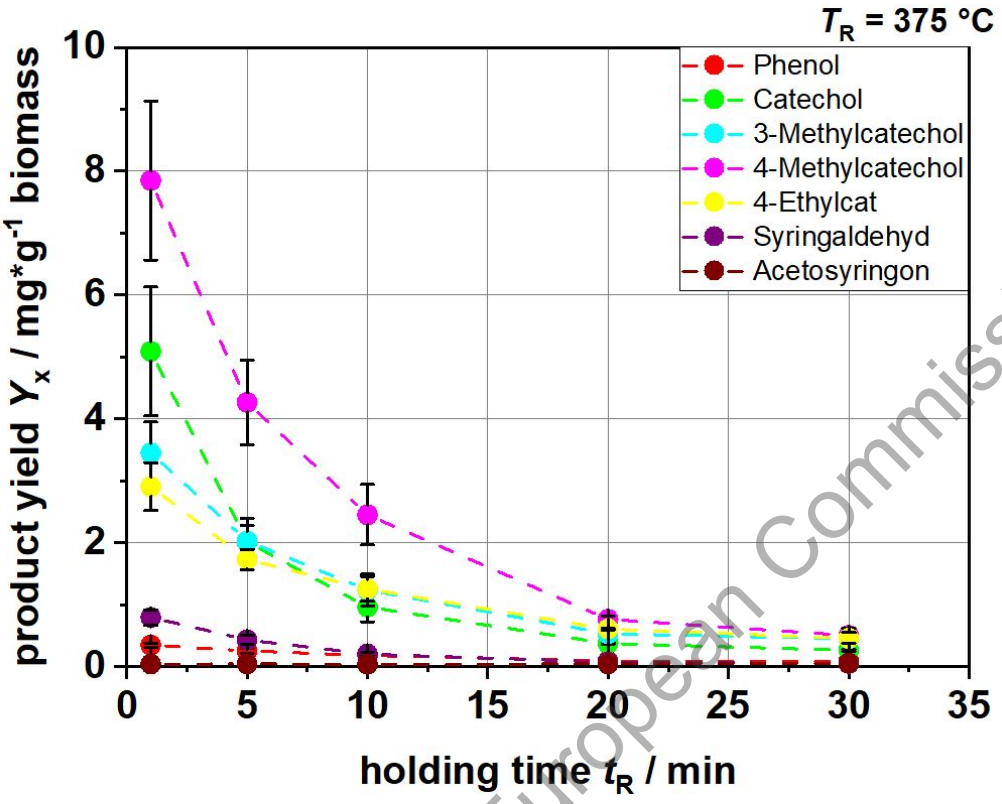

Figure 7: Product yields of aromatic compounds after HTL of black liquor; t_R = 1 – 30 min; T_R = 375 °C

Next, we took a closer look at the aromatics that could be extracted from the liquid product phase. From the results presented above, we developed a simple reaction scheme (see **Figure 8**). This scheme can serve as a basis for subsequent modeling work for a reaction kinetic model. Starting from lignin as feedstock, intermediates such as syringol and its derivatives are formed first. However, guaiacol as well as 3-methoxycatechol are also distinct intermediates. These substances then react further during the HTL process to form the actual products such as catechol. As mentioned before, we assume that a large part of the aromatics reacts further via coking and repolymerization reactions and ends up in the solid. The other part forms the typical components in the gas phase such as CO_2, H_2 and hydrocarbons. What is striking is the difference between hardwood (e.g., eucalyptus wood, project feedstock) and softwood (e.g., softwood) as the basis for the lignin or black liquor. Previous work by Schuler et al. [8, 9] addresses the HTL of extracted lignin, more specifically Indulin AT. This feedstock is extracted from softwood. In contrast to the results in this deliverable, the yields of phenol and guaiacol in Schuler's work are significantly higher. Phenol is also classified there as one of the main products. The reason for this probably lies in the differences in the nature of softwood and hardwood. While the former is almost exclusively composed of a phenyl propanoid, coniferyl alcohol, the latter also has a high proportion of sinapyl alcohol. **Figure 9** shows the two different molecules. It can be clearly seen that sinapyl alcohol mainly forms syringol and its

derivatives, whereas this is not possible with coniferyl alcohol. How far this is related to the yields of catechol and phenol must be investigated in further work.

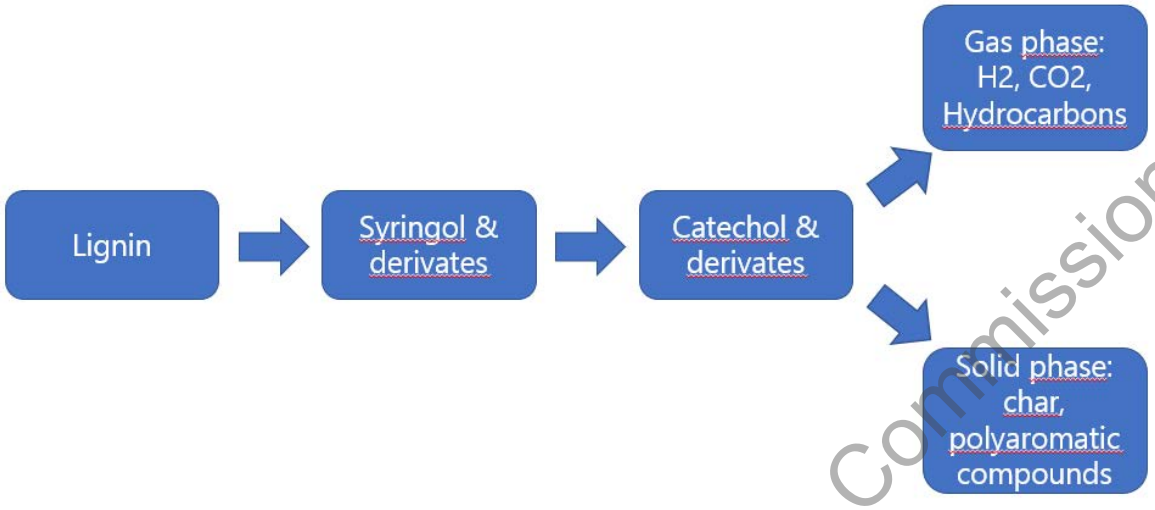

Figure 8: Simple reaction pathway based on results of the experimental studies

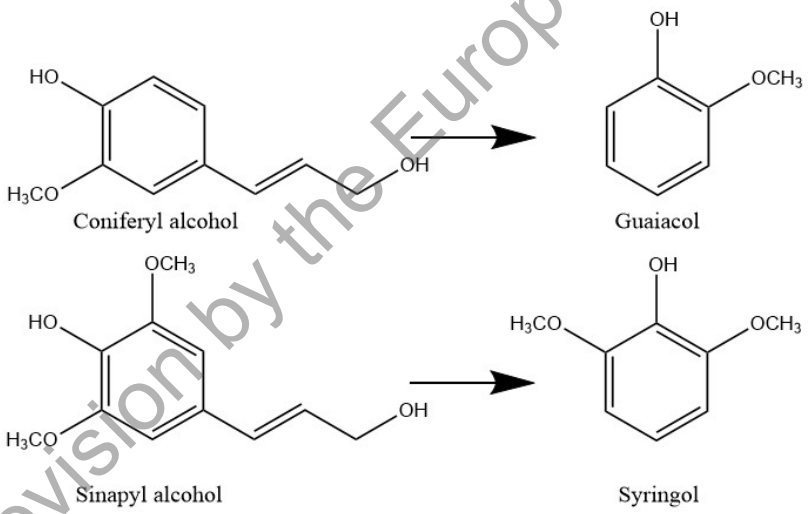

Figure 9: main phenyl propanoids, coniferyl alcohol & sinapyl alcohol, (left) and their monomer compounds, guaiacol & syringol as intermediate in the product (right)

2.2.3 Biocrude yields and molecular weight analysis

To get a more complete picture of the HTL process, it is important to look at more than just the monomers. Our assumption is that not only monomers are split off from the lignin molecule, but also smaller and larger oligomers in parallel. Smaller molecules can then also subsequently form from these molecules (see **Figure 10)**. With GC analysis, only part of the organic product phase can be determined. Larger compounds cannot be brought into the gas phase because the boiling temperatures are too high, which means that they are not detected.

To have a clue about the progress of depolymerization as well as possible repolymerization effects, it makes sense to look at the molecular weight.

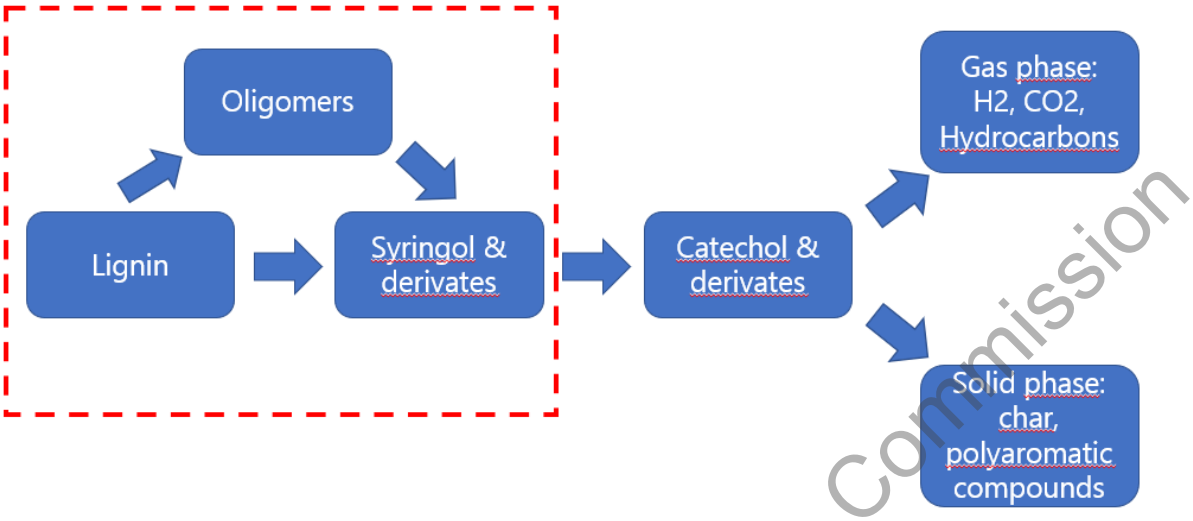

Figure 10: Assumed reaction pathway with additional step (oligomers) inside

First, the Biocrude yields with the described extraction procedure are shown. These confirm the low organic carbon content of the liquid product phase in the mass balance. However, the dependency is not the same. One possible reason for this could be the presence of volatile compounds. **Figure 11** and **Figure 12** show the respective biocrude yield results for different reaction temperatures and holding times. In the relevant parameter ranges, the yield is between 5 - 10 wt. % or even lower, which is very low compared to other studies [10, 11]. An exception is the yield at T_R = 250 °C. However, this value should be treated with caution, since at low temperatures the depolymerization of the lignin is not yet so advanced. Another problem with the extraction and analysis of the biocrude is the very small amounts of feedstock as well as product due to the experimental design. Analyses were performed only to a very limited extent for this reason, as the susceptibility to errors was too high due to the small quantities. Extraction of the products at 400 °C was not possible. Significantly, better results are expected as part of the continuous trials. The focus will then be increasingly on biocrude extraction as well as its analysis.

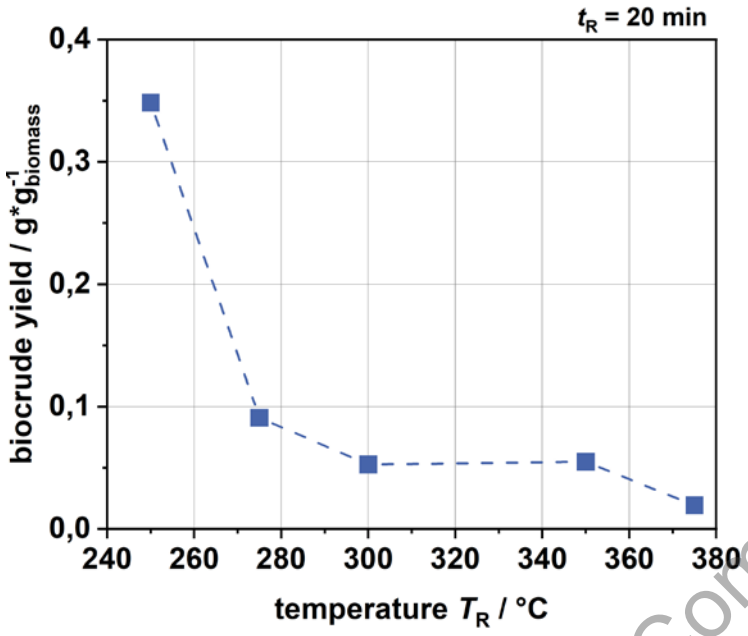

Figure 11: biocrude yields after extraction with ethyl acetate; T_R = 250 – 375 °C; t_R = 20 min

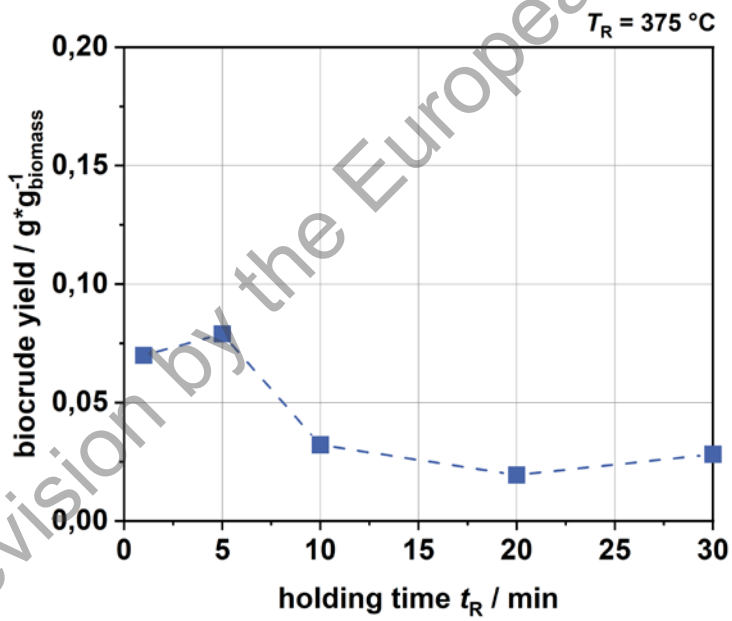

Figure 12: biocrude yields after extraction with ethyl acetate; t_R = 1 – 30 min; T_R = 375 °C

To determine the molecular weight as a description of the depolymerization process, we selected the extracted biocrude. Since only a small amount of sample is needed for analysis by SEC, this was not a problem. The molecular weight was averaged for all samples within the calibrated range (246 g/mol – 20000 g/mol). Polystyrene sulfonate sodium salt was used as calibration standard. The molecular mass average was calculated with respect to the calibration curve. It should be noted that the results only approximate the molecular weight. Due to the properties of lignin, it is difficult to make statements about the absolute values, as already

mentioned in chapter 2.1.3. Nevertheless, conclusions on the depolymerization of the lignin can be drawn mainly from the relative course. **Figure 13** shows the average molecular weight *M* of the biocrude at different temperatures. The diagram also shows the molecular weight of the lignin (pink). It should be noted that part of the signal of the lignin sample is outside the calibrated range. Therefore, it can be assumed that the molar mass of the lignin is still higher than indicated in the figure. The same is true for the point at T_R = 250 °C, but to a much lesser extent. It can be clearly seen how the molecular weight decreases with increasing reaction temperature. From T_R = 300 °C and a molecular weight *M* of about 4000 g/mol, no further decrease can be observed. Instead, the value remains stable. A possible reason for this could be an equilibrium between depolymerization and repolymerization reactions. Another possible reason could be the non-consideration of molecules outside the calibration range. The same phenomenon can be observed in **Figure 14** at different holding times t_R. Here, as well as in the other figure, the molar mass of the biocrude does not decrease further after 10 minutes, while a clear decrease can be observed for the lignin at the lower holding times.

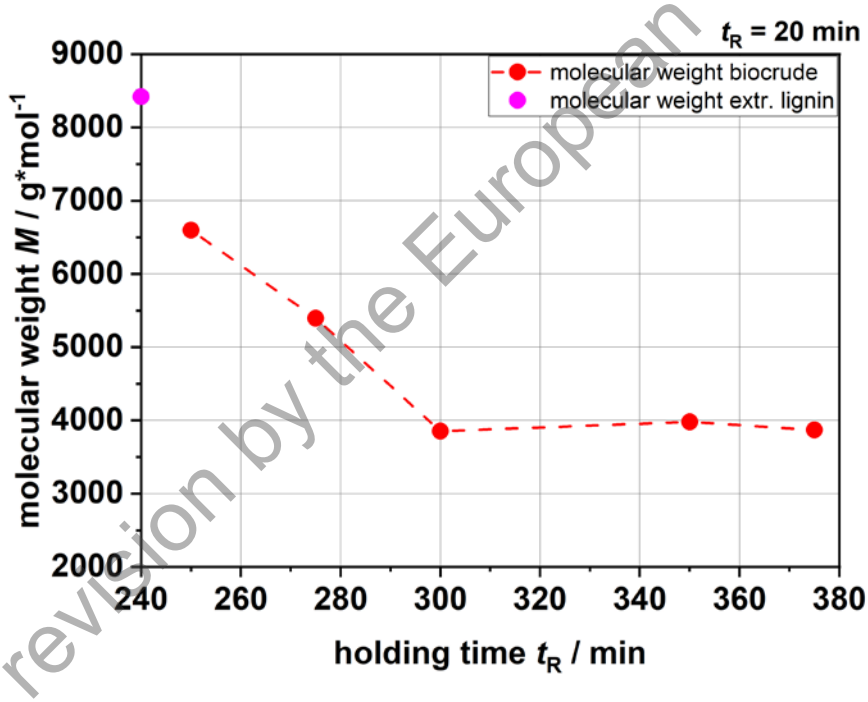

Figure 13: average molecular weight M of extracted biocrude; T_R = 250 – 375 °C; t_R = 20 min; pink dot: extracted hardwood lignin

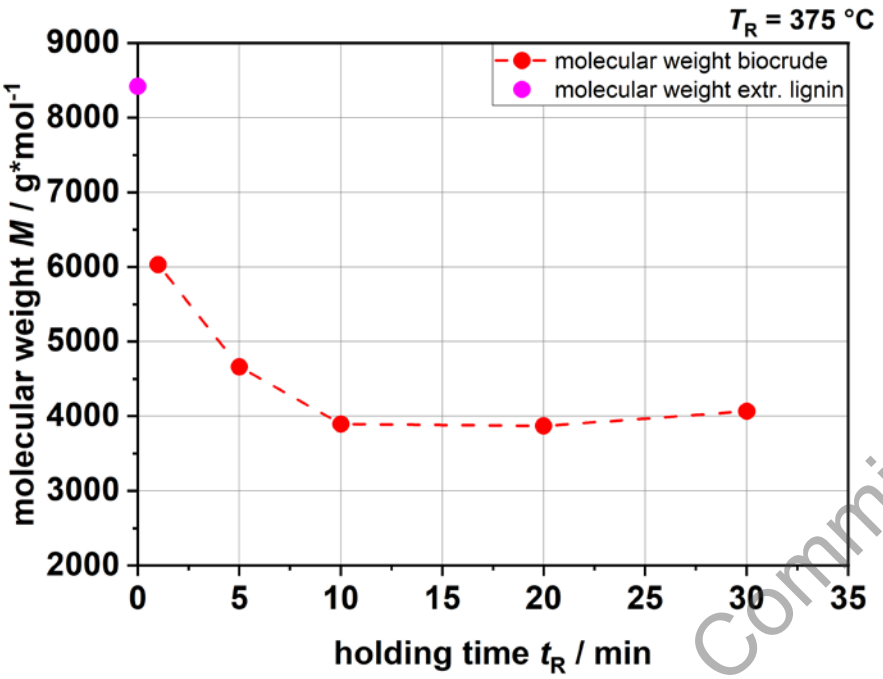

Figure 14: average molecular weight of extracted biocrude; t_R = 1 – 30 min; T_R = 375 °C; pink dot: extracted hardwood lignin

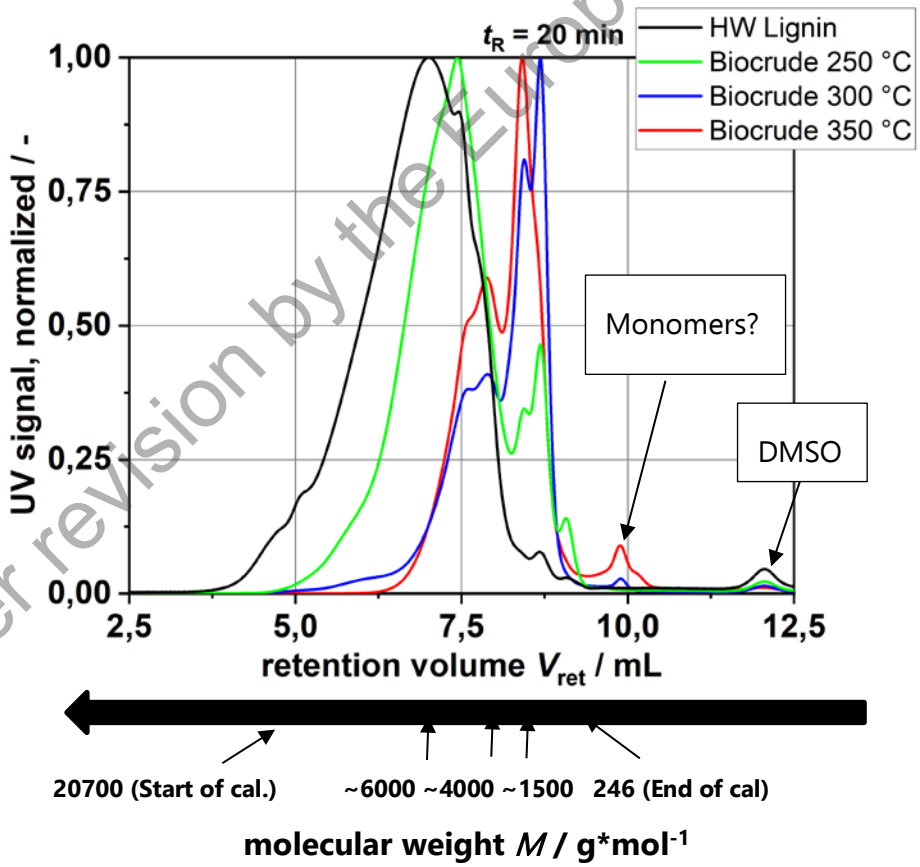

Figure 15: SEC chromatograms of different biocrudes from reaction temperature variation; molecular weight decreasing with higher retention volume

Figure 15 and **Figure 16** show the chromatograms of individual samples. It shows the UV signal of the detector versus the retention volume V_{ret}. The retention volume is the volume transported through the column and correlates with the retention time. The molecular weight is in reverse order and is not linear. The calibration curve is proportional to $-x^3$. The smaller the molecule, the more it interacts with the stationary phase of the SEC column. This leads to a longer retention time in the column which results in a higher retention volume. This is only a qualitative analysis. Therefore, the chromatograms have been normalized for better illustration. At higher temperatures and holding times, different peaks occur at certain molecular weights. Basically, a shift of the peak peaks towards lower molecular weights can be seen in both diagrams. Furthermore, new peaks appear at a molecular weight of about 1500 g/mol, which leads to clearly pronounced double peaks within the calibration limits. It can also be seen that the chromatograms at T_R = 300 °C and higher and t_R = 10 min and higher no longer show any major differences. This leads to the stable average molecular weight for just these samples. At a retention volume V_{ret} = 10 ml, a peak is formed which increases with increasing reaction temperature T_R and holding time t_R. This is below the calibration limit of 246 g/mol. It is at highest at t_R = 30 min in **Figure 16** (red) compared to the other peaks at higher molecular weights. These could be monomers, which would make sense from an estimated molecular weight between 100 - 200 g/mol. However, this is contradicted by the fact that at higher temperatures we could hardly find any aromatic monomers in the liquid phase by GC-FID. Possibly these are components that cannot be detected with the configuration of the GC. The relationship still needs to be understood at this point. These peaks don't explain the barrier at 4000 g/mol neither. Only the peak at t_R = 30 min outside of the calibration range could have a significant influence on the average molecular mass. The others are very small compared to the other peaks of the chromatogram. Regarding **Figure 10**, it can be stated that the step via the oligomers is occurring in the depolymerisation reaction. This is made visible by the formation of new peaks in the chromatogram. If only monomers and small components were to split off permanently, the chromatogram would have to shift to the right without changing much. Since this is not the case, we assume that larger oligomers are formed, which can then presumably also react further. What is also visible from the SEC analysis is that despite the HTL, there are still lignin residues with a high molecular weight. These cannot be further reduced in the investigated area.

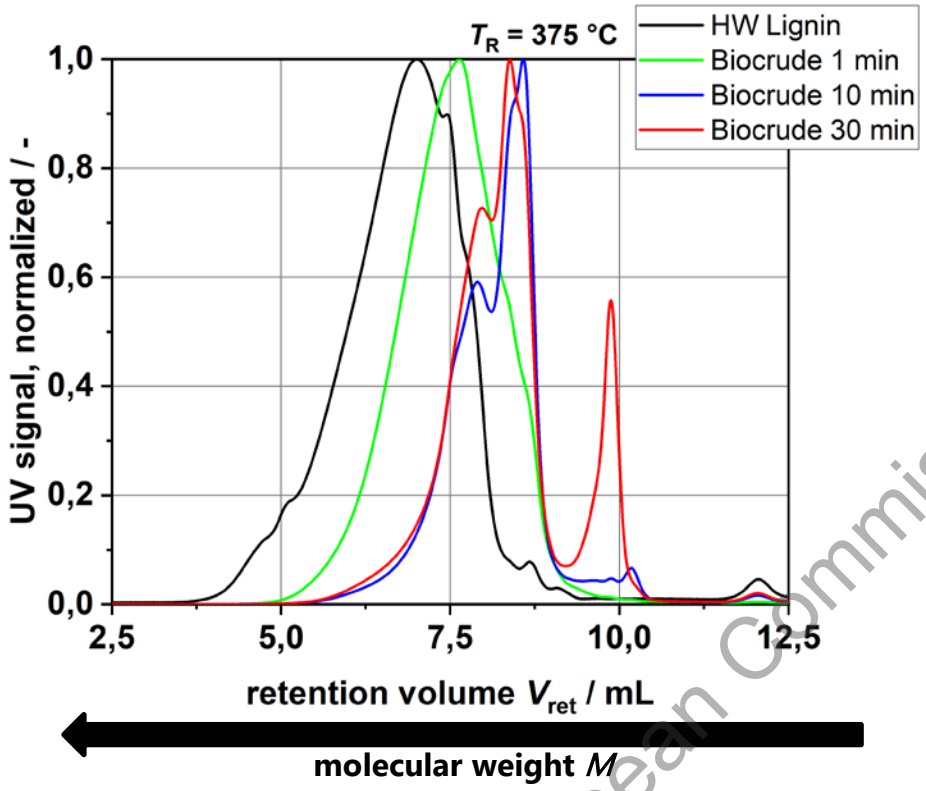

Figure 16: SEC chromatograms of different biocrudes from holding time variation; molecular weight decreasing with higher retention volume

At last, the results of the HPLC analysis are shown in **Figure 17** and **Figure 18**. These are plotted as concentration versus reaction temperature T_R and holding time t_R. The point at T_R = 275 °C couldn't be analysed due to an experimental error. As expected, the concentrations of the multifunctional acids decrease in both figures. Interestingly, in both cases the concentration of acetic acid is increasing. Also notable are the maxima at T_R = 300 °C for the two alcohols. Afterwards both concentrations are decreasing. Regarding the two acids, formic acid and acetic acid the behavior could be explained by their different stability in the process conditions. Formic acid tends to decompose to CO_2 and H_2 whereas acetic acid is rather stable. The HPLC analysis was made with our state-of-the-art analysis setup. To go deeper into the aqueous phase analysis an HPLC-MS would be needed to do some qualitative analysis to find more compounds. With our setup, it is only possible to compare undefined peaks with reference substances and look for a match for the two peaks.

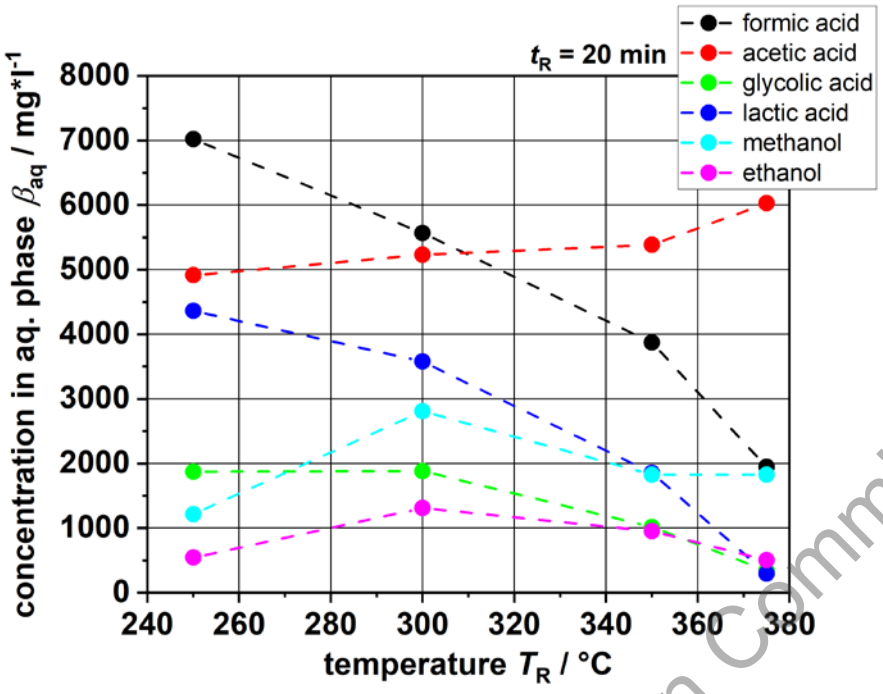

Figure 17: concentration in aq. phase after organic phase extraction for calibrated acids and alcohols; ; T_R = 250 – 375 °C; t_R = 20 min

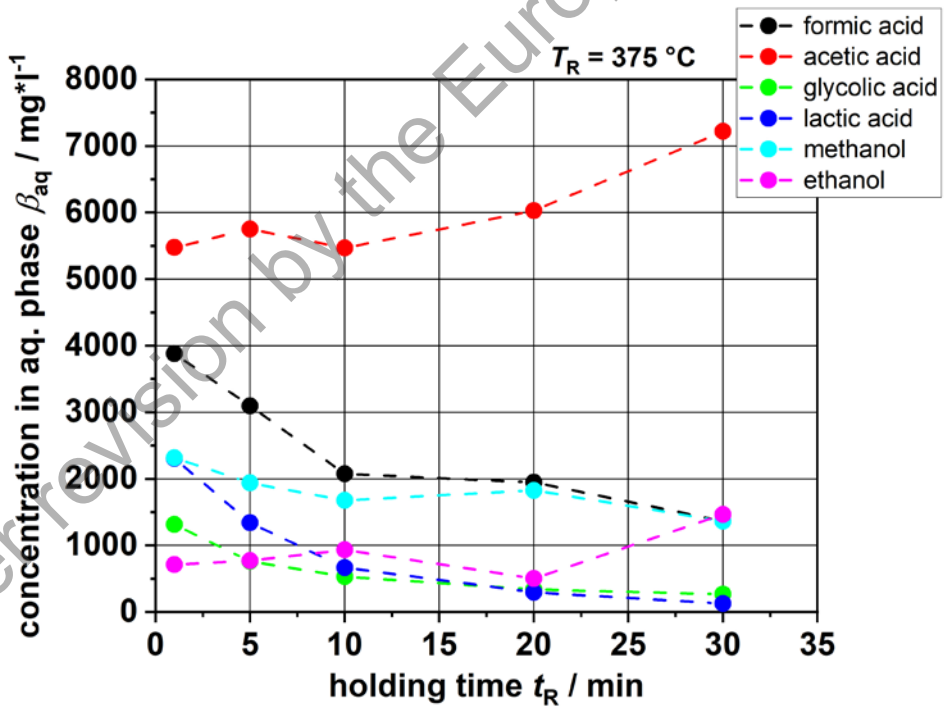

Figure 18: concentration in aq. phase after organic phase extraction for calibrated acids and alcohols; t_R = 1 – 30 min; T_R = 375 °C

3 Influence of the cooking chemicals on the HTL process

An important question in the study of HTL of black liquor is the behavior of the various cooking chemicals required for the Kraft process. Especially sulfide, which is mainly used as sodium sulfide in the paper industry, is very reactive . One possible product is hydrogen sulfide (H_2S), a very toxic and corrosive gas. Another problem is the possible formation of organosulfur compounds. These are formed by reactions of inorganic sulfur salts with organic compounds. While inorganic sulfur-containing compounds are relatively easy to remove from the products, organic sulfur compounds are more difficult to remove. This leads to problems with the necessary catalysts in the course of the process chain, especially the upgrading steps of the biocrude as well as the Aqueous Phase Reforming (APR). The organo-sulfur compounds can lead to catalyst fouling and deactivation, which drastically reduces the conversion rates. To avoid this, it is therefore important to use countermeasures such as sulfur-resistant catalysts. In order to be able to take more targeted action against this, it is important to know as much as possible about the sulfur compounds present and their concentration.

This report is mainly limited to the influence of sulfide since it is the most reactive one and pre-experiments with sulfate do not show mentionable impact. Experiments are currently underway to show the difference between carbonate and hydroxy ions, and sodium or potassium as the corresponding cation. These experiments have not yet been completed at the time of publication of this report and will therefore not be described in further detail. Additionally, we have also observed the behavior of sulfur during the real BL experiments. For this purpose, we checked all the phases for sulfur or sulfur compounds. This helps us to get a clear picture where the sulfur will stay after the HTL process

3.1 Materials and Methods

The influence of the cooking chemicals on the HTL process was carried out in the micro autoclaves of the same design as the previously described series of experiments. The handling is exactly as described in **chapter 2.1.2**.

3.1.1 Preparation of the model black liquors

The feedstock is a significant factor in the difference. In order to be able to determine the influence of the cooking chemicals, the different salt concentrations must be known. For this reason, we decided to produce model liquors that are as close as possible to the actual black liquor. For this purpose, we first prepared a salt solution containing the most important components.

The different salt concentrations were determined by ion chromatography (IC), ICP-OES and TIC as part of the feedstock characterization. The sulfur-containing anions, sulfate (SO_4^{2-}), sulfite (SO_3^{2-}), thiosulfate ($S_2O_3^{2-}$) as well as (bi-)sulfide (HS^-/S^{2-}) could be determined by IC (In the further course, only bisulfide (HS^-) will be mentioned, since the equilibrium in the present

matrix, pH value of 12 - 13, is almost completely on its side). It should be mentioned here that with our technical possibilities the bisulfide concentration could not be quantified directly. To determine the concentrations, the HS^- or S^{2-} ions were first precipitated by means of iron(II) chloride. In the next step, IC analysis was used to quantify the other sulfur-containing salts. The sulfide concentration could then be determined by calculation (see **chapter 3.1.2**). The carbonate content (CO_3^{2-}) was set equal to the inorganic carbon in the black liquor, which was determined via a TIC measurement. The concentrations of the cations sodium (Na^+) and potassium (K^+) were determined by ICP-OES analysis. A component list with the corresponding concentration was then drawn up from all the data obtained with regard to the feedstock. Attention was paid to accurately include as much of the analytical results as possible. They are presented in **Table 7**. The salts were dissolved in 100 mL of distilled water. In the next step, hardwood lignin was added to the salt solution with stirring. The lignin was extracted lignin from the black liquor used for the other experiments. The Navigator Company provided us with several hundred milligrams of lignin for this purpose. They performed the extraction in their laboratories. **Table 8** shows the results of the EA and ICP-OES analysis of the dried extracted lignin. The amount of dissolved lignin is also in **Table 7**. We based our analysis on the value of the dried mass $w_{tr,waf}$ from the feedstock analysis, which was free of water and ash. Since our focus is on the depolymerization of lignin, we neglected other organic components such as hemicellulose and defined the complete organic matter as lignin.

	Na_2CO_3	K_2CO_3	Na_2SO_3	Na_2SO_4	$Na_2S_2O_3$	Na_2S	Lignin
concentration / g*l^{-1}	16,94	2,63	1,3	1,04	1,9	7,3	90,0

Table 7: concentration of salts and lignin in the model black liquor

The prepared model black liquors were then purged with nitrogen and stored in a fridge. A total of four model liquors were prepared with the aim of investigating the behavior of the sulfur-containing salts and their influence on the HTL using bisulfide (HS^-) for example. For this purpose, the bisulfide concentrations of 0 g*l^{-1}, 1 g*l^{-1}, 2 g*l^{-1} and 3 g*l^{-1} were set. We decided that all experiments are done at T_R = 375 °C and t_R = 10 min.

Element symbol	Mass fraction in dry mass / wt. %
C (EA)	60,3
H (EA)	5,7
N (EA)	< 0,1
S (EA)	2,6
O (Diff.)	31
Na (ICP)	0,4
K (ICP)	< 1

Table 8: Elemental analysis and ICP results for extracted and dried Lignin used for the model BL; oxygen calculated by difference

3.1.2 Additional analytic methods

The analytical procedures for the examination of the products of the HTL of the model liquors is mostly identical. This applies both to the sample preparation and to the analyses themselves. The detailed descriptions can be found in **chapter 2.1.3**. Further analyses were carried out or existing ones were extended in order to obtain more detailed information on the sulfur and its compounds.

To determine the amount of sulfur in the solid, we used the elemental analysis. The liquid product phase was analyzed for total sulfur content by ICP-OES. An aliquot of the liquid phase was taken and diluted to 1:100. The dilution was prepared using 0,1 mL of sample, 0,5 mL of hydrogen peroxide (H_2O_2), 1 mL of potassium hydroxide (KOH), and 8,4 mL of purified water. The H_2O_2 oxidizes the inorganic sulfur compounds to sulfate, in which molecule the sulfur reaches the highest oxidation state. This is true for all inorganic sulfur salts present in our system. For some this occurs more rapidly (HS^-) for others more slowly ($S_2O_3^{2-}$) [12]. The addition of KOH provides a more stable alkaline environment that catalyzes the oxidation process with H_2O_2. After 24 hours, no other peaks could be detected by IC analysis except for the sulfate peak. This was quantified by the mass concentration β_{SO42-}. Assuming that any inorganic sulfur in the sample is bound in the sulfate now present, the mass fraction of inorganic and organic sulfur in the sample can be calculated from this. This procedure is based on the publication of Jeyakumar et al. [13], which is used to determine the sulfide concentration. For the characterization of the feedstock, the sample was treated in the same way. The sulfur components of the measured salt concentration after precipitation of the sulfide are subtracted from the total inorganic sulfur. Assuming that no other inorganic sulfur compounds are present, the difference must correspond to the concentration of the sulfide.

To determine the mass fractions of organic and inorganic sulfur, the molar concentration c_{SO42-} must first be calculated.

$$c_{SO_4^{2-}} = \frac{\beta_{SO_4^{2-}}}{M_{SO_4^{2-}}} \quad (7)$$

For this, the measured mass concentration is divided by the molar mass of sulfate M_{SO42-}. In the next step, the mass concentration is multiplied by the molar mass of sulfur M_S to obtain the mass concentration of sulfur β_S.

$$\beta_{S,inorg} = c_{SO_4^{2-}} * M_S \quad (8)$$

The difference between the total sulfur concentration in the liquid sample, which was determined by ICP analysis leads to the organic sulfur concentration.

To determine individual organic sulfur components in the liquid, the Paul-Scherrer-Institute (PSI) provided a GC with a sulfur chemiluminescence detector (SCD). Before analysis, 0,5 mL of the liquid sample was dissolved in 1,5 mL of isopropanol and filtered.

For gas analysis, we first attempted to qualitatively determine various typical organic and inorganic sulfur compounds. In the end, it quickly became apparent that hydrogen sulfide (H_2S) and dimethyl sulfide (DMS) were relevant. For the analysis, we used a GC (GC 7890B, Agilent) with a column specially made for sulfur compounds (RT-U-Bond, Restek). Additionally, after initial corrosion problems, the inlets and liners of the GC had to be replaced with components with a higher resistance against the sulfur compounds. Both materials were calibrated to make quantification possible. For the DMS, which is a liquid under normal conditions, T_{boil} = 36 °C, the calibration was performed by headspace method. For this purpose, DMS was mixed with methanol in different amounts in a closed system with a septum. Using a gas injection syringe, the gas phase could be withdrawn above the liquid level and transferred to the GC. Using the vapor pressure and the ideal gas law, the concentration of DMS in the closed vessel could be determined. Since the vapor pressure curve depends only on the temperature or on a second component in the system, we used methanol to vary the DMS concentration without having to change the temperature.

3.2 Results and discussion

3.2.1 Behavior of sulfur during the HTL process

3.2.1.1 Liquid and solid phase analysis

First, we looked at the behavior of the sulfur during the HTL process. **Figure 19** and **Figure 20** show the different sulfur mass concentrations in the liquid, filtered product phase at different reaction temperatures T_R and holding times t_R. The sulfur concentration in organic compounds has been calculated by the difference of the other two. **Figure 19** clearly shows that the total sulfur concentration $\beta_{S,total}$ clearly decreases with increasing temperature T_R. This is clearly visible in the lower temperature segment. From T_R = 325 °C on, the decrease in total sulfur concentration is less pronounced. In contrast, the inorganic fraction decreases only slightly over the entire temperature range and even remains largely constant in the right half of the diagram. However, even the small decrease in the inorganic sulfur concentration indicates a direct participation of the inorganic sulfur salts in the depolymerization reactions. The sulfur-containing organic compounds formed are probably highly volatile or gaseous. This can be justified by the sharp decrease in the organic sulfur concentration in the liquid phase. When compared with the investigation of the sulfur concentration at different holding times t_R, it is notable that an increase in the holding time does not lead to a clear increase or decrease. An exception is the experiment at t_R = 30 min, where a strong increase can be observed. Whether this is true, or whether it is a measurement error at this point, must still be investigated in a repeat experiment. It is clear that the temperature has a much greater influence on the behavior of the sulfur compounds during the HTL process than the holding time. In addition to faster reactions, such as the inorganic salts with the organic material in the process, the near or supercritical environment probably also plays a role. In studies of the holding time, the pressure and temperature components that are decisive for this are kept constant, which is of course not the case when the reaction temperature is varied. Due to the strong change in water properties with increasing temperature, it can be assumed that this also influences the depolymerization reactions.

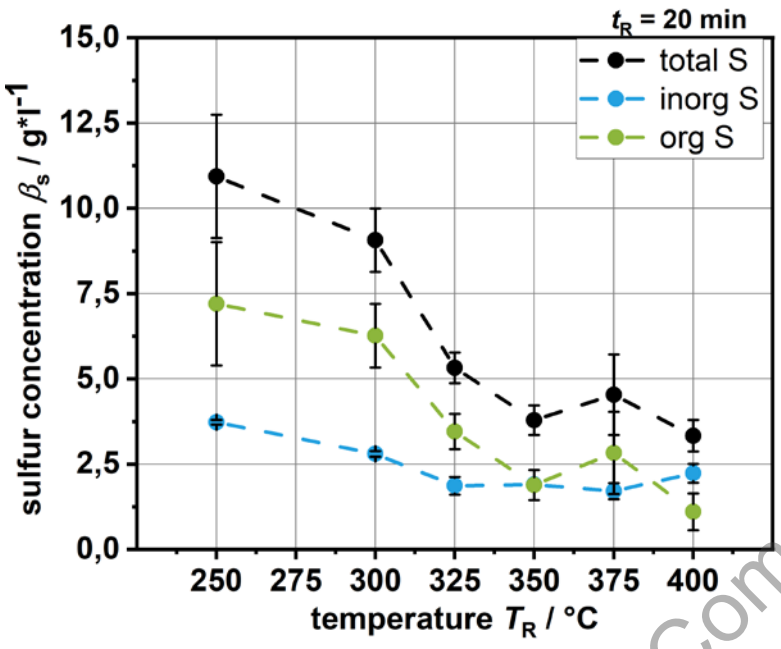

Figure 19: sulfur mass concentration β_S in liquid product phase at different reaction temperatures T_R; black: total sulfur in liquid phase (ICP-OES analysis); blue: inorganic sulfur in liquid phase (IC analysis & calculation); green: organic sulfur in liquid phase (calculation, difference between total S and inorganic S); raw BL: total S: 15,2 g*l^{-1}; inorganic S: 4,89 g*l^{-1}; organic S: 10,31 g*l^{-1}

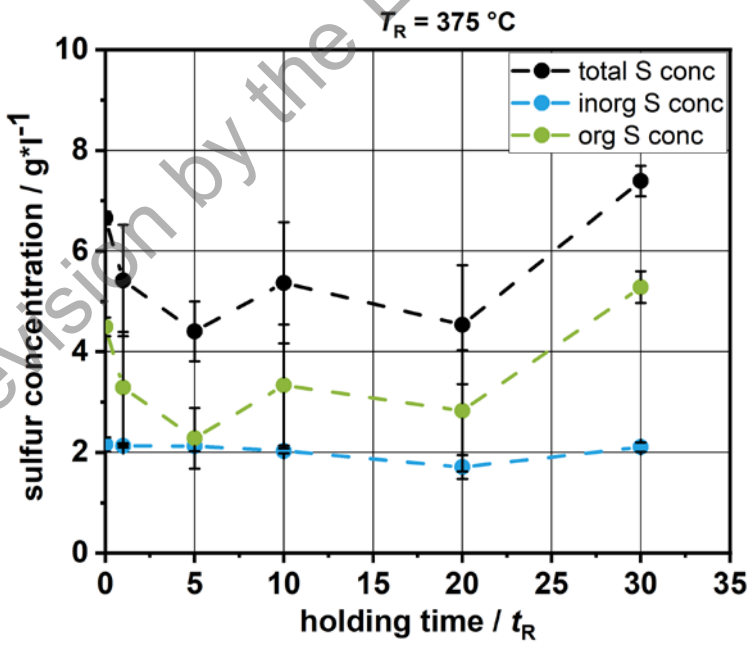

Figure 20: sulfur mass concentration β_S in liquid product phase at different holding times t_R; black: total sulfur in liquid phase (ICP-OES analysis); blue: inorganic sulfur in liquid phase (IC analysis & calculation); green: organic sulfur in liquid phase (calculation, difference between total S and inorganic S); raw BL: total S: 15,2 g*l^{-1}; inorganic S: 4,89 g*l^{-1}; organic S: 10,31 g*l^{-1}

Nevertheless, the question arises in which product phases the sulfur ends up. It can be assumed that we can almost completely represent the total sulfur concentration in the liquid phase with the ICP-OES analysis. The solid phase has a stable amount of 4 – 8 wt. % of the total sulfur over all measuring points (see **Figure 21**) without a clearly visible tendency. This is not sufficient to explain a decrease from above 10 to below 5 g/L sulfur in the liquid product phase. In the following chapter, therefore, the gas phase was investigated in more detail in order to better elucidate the fate of the sulfur.

Before discussing the results of the gas phase analysis, the sulfur-containing products in the liquid phase will be discussed in more detail. A handful could be qualified by GC-SCD. However, with the exception of dimethyl sulfide (DMS), dimethyl disulfide (DMDS), and dimethyl trisulfide (DMTS), all other detectable substances were below the calibration limit or too volatile to perform reasonable quantitation. The three substances are all organic sulfides (see **Figure 22**). The components that could only be determined but not quantified were, on the one hand, other diverse sulfides such as ethyl sulfide. On the other hand, simple mercaptanes such as methyl mercaptan and ethyl mercaptan could also be detected. In addition, one peak of thiophene could be assigned.

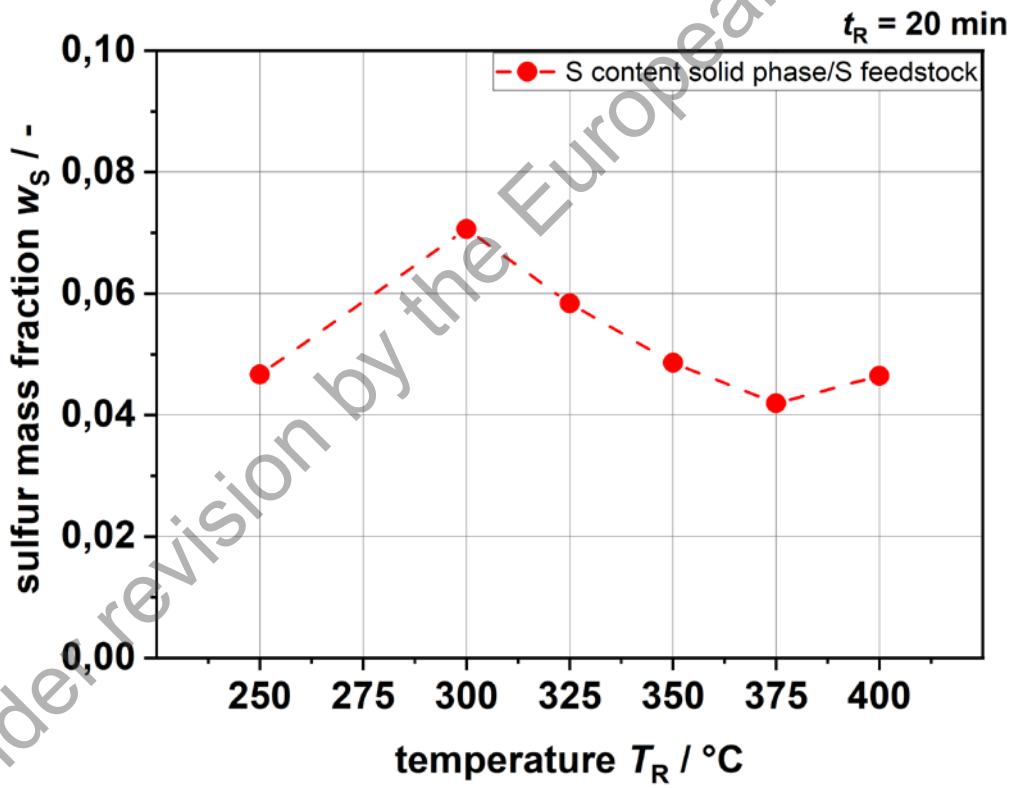

Figure 21: mass fraction w_S of sulfur in the solid phase related to total sulfur in the feedstock

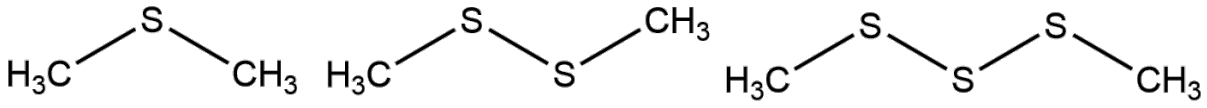

Figure 22: The three organic sulfides quantifiable via GC-SCD analysis (DMS left; DMDS middle; DMTS right)

Figures 23, 24, 25 and 26 show the mass concentrations of DMS and of DMDS and DMTS, respectively, for the different reaction temperatures T_R and holding times t_R. It can be seen immediately that DMS is the main component of organic sulfur substances in the liquid phase. The concentration is compared to the other two ten times higher. At the various reaction temperatures, a similar tendency to the organic sulfur content in the liquid phase can be seen for all three substances. At higher temperatures, the value decreases in each case. An exception is the point at T_R = 400 °C. Here, the DMS concentration decreases extremely, while the DMDS concentration increases a little bit. A possible explanation for this has not yet been found. Interestingly, the sulfur from these three components is far from sufficient to achieve the values of total organic sulfur. Due to this observation, it seems that other sulfur compounds must be present. It could be possible that most of the organic sulfur is present in bigger molecule structures like we already saw in the SEC analysis. This would also fit with the results of the analyses at different holding times. In contrast to the total organic sulfur, which did not show a clear trend, the DMS concentration decreases steadily with longer holding times. The concentrations of the other two sulfides, DMDS and DMTS, also decrease first and then slowly increase. To fill this gap, other measurement methods must be used. It is possible that an analysis using HPLC-HRMS could provide even more information about the molecular structures as well as the fate of the sulfur.

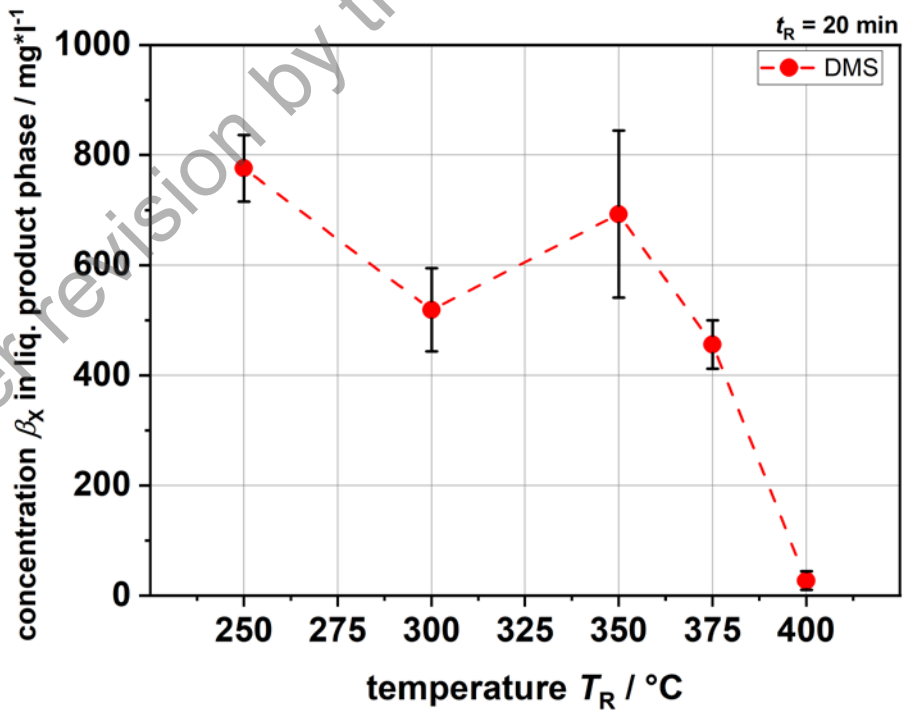

Figure 23: DMS concentration in liquid product phase at T_R = 250 - 400 °C; t_R = 20 min; GC-SCD analysis

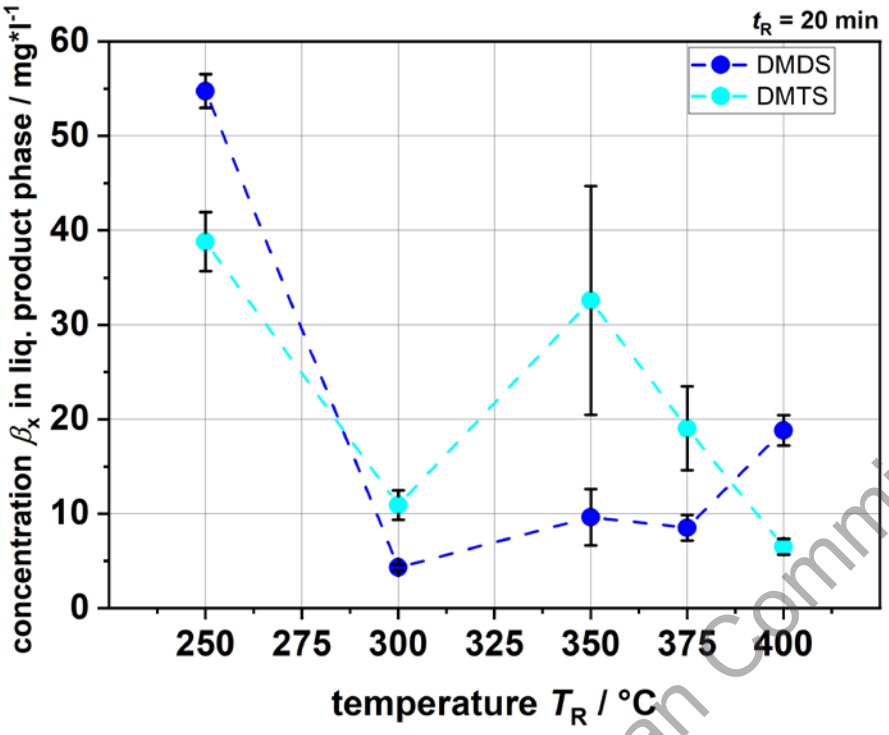

Figure 24: DMDS/DMTS concentration in liquid product phase at T_R = 250 - 400 °C; t_R = 20 min; GC-SCD analysis

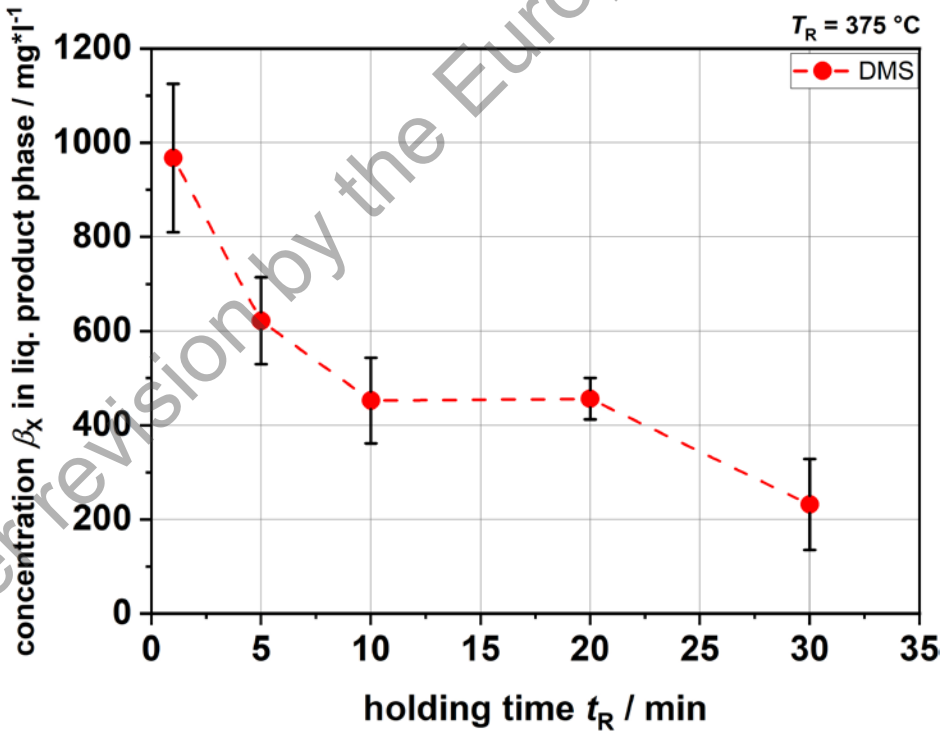

Figure 25: DMS concentration in liquid product phase at t_R = 1 – 30 min; T_R = 375 °C; GC-SCD analysis

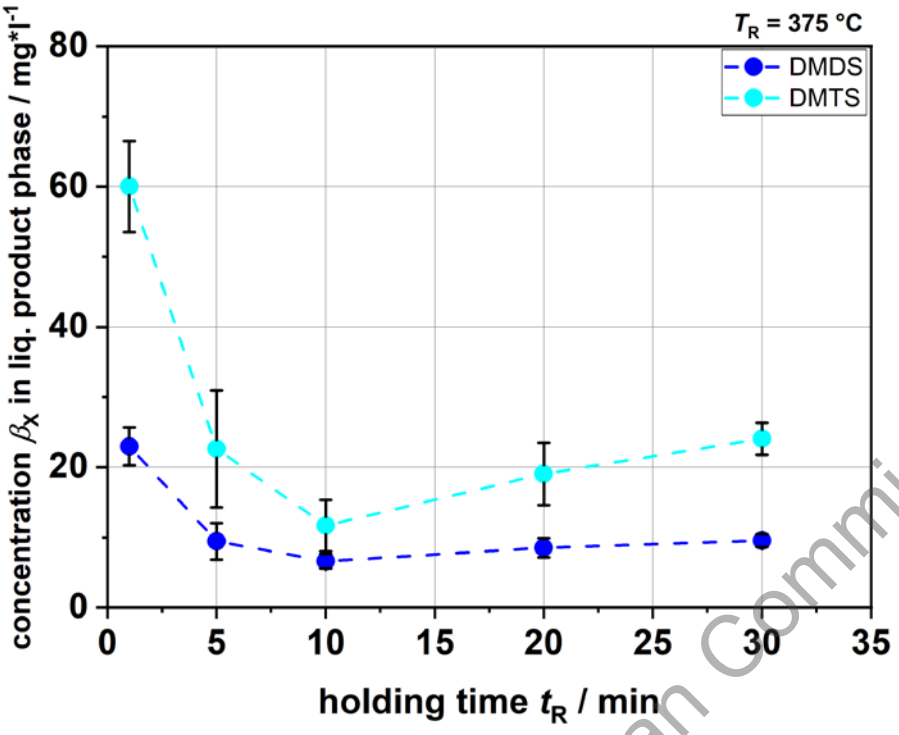

Figure 26: DMDS/DMTS concentration in liquid product phase at t_R = 1 – 30 min; T_R = 375 °C; GC-SCD analysis

3.2.1.2 Gas phase analysis

To see if significant amounts of sulfur end up in the gas phase during the HTL process, we decided to investigate it more closely. Since it was not possible for us to directly measure the sulfur content in the gas phase, we had to look for specific sulfur-containing gaseous compounds in the product. The most logical idea is that hydrogen sulfide (H_2S) is formed during HTL. Sulfides are salts of H_2S. The three states of the compound (H_2S, HS^-, S^{2-}) are in equilibrium as explained in the previous chapter and are largely dependent on the pH value. The pH value decreases during HTL. Measurements on this have confirmed that the liquid product phase has a pH value of 8 – 11 (see **Figure 29**). Assumingly the pH decreases due to production of CO_2, which reacts with the OH- in the liquid phase to form carbonate. Thus, the slight shift of the equilibrium towards H_2S inevitably produces it. H_2S could also be produced via reactions. To cover also organic compounds, we analyzed a gas sample by GC-MS. The chromatogram is shown in **Figure 27**. One peak clearly stands out. Both the National Institute of Standards and Technology (NIST) database on file and a check using the pure substance on GC-FID confirmed that this is again dimethyl sulfide (DMS). Compared to all other detected substances by GC-MS, this peak is by far the largest. Otherwise, mainly various cycloalkanes and cycloalkenes were found. The second larger peak, the double peak before the DMS peak, could not be assigned exactly, because the method used as well as the setup is not designed for gaseous substances (DMS liquid at room temperature, boiling point T_{boil} = 36 °C). It is most likely that one part of the double peak is methane mercaptane. Furthermore, according to the NIST database, thiophene and other organic sulfides and disulfides are still in the gas phase. The peaks are very small. Hydrogen sulfide could not be found.

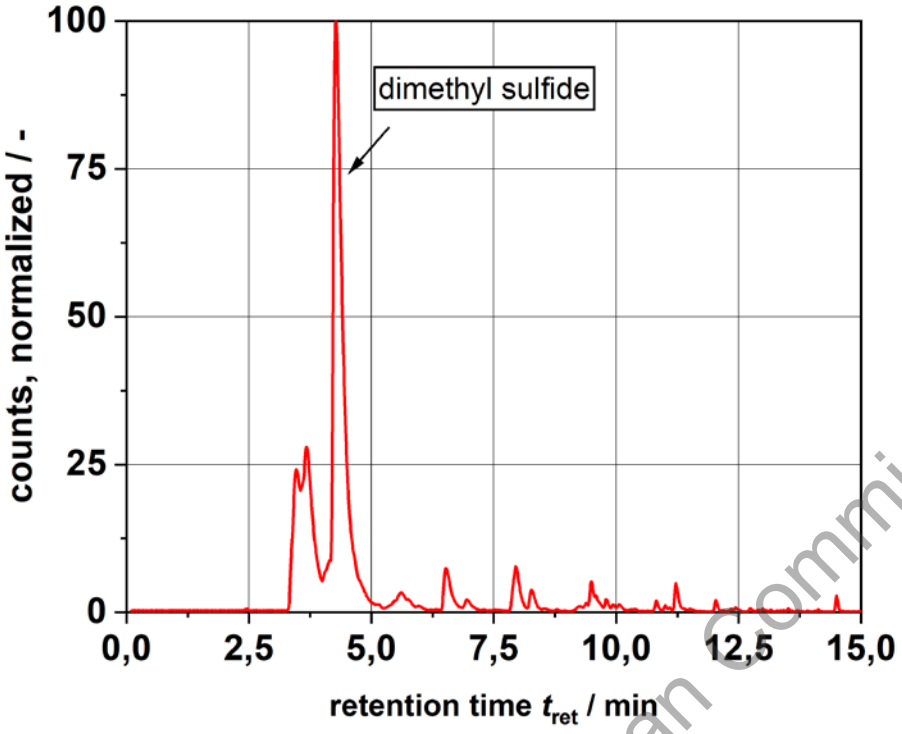

Figure 27: GC-MS chromatogram of a gas sample from an HTL batch experiment (T_R = 375 °C, t_R = 10 min)

As already mentioned, we were also able to qualify the presence of DMS in the gas phase by means of GC-FID. Furthermore, as described in **chapter 3.1.2**, we succeeded in performing a quantification. In addition to quantifying the volume fraction of DMS $\phi_{DMS,gas}$, we were also able to accurately determine that of H_2S $\phi_{H2S,gas}$ in the gas phase. These results are shown in **Figure 28**. Due to the difficulties in calibration as well as general technical difficulties in gas analysis, only the gas samples of the samples at different reaction temperatures T_R as well as the model liquors have been performed. It should be noted that the graph does not take into account the different amounts of feedstock. These mainly affect the point at T_R = 400 °C. From the plot of the volume fraction of H_2S in the gas sample, a clear slope can be seen with the exception of the point at T_R = 400 °C mentioned above. This course coincides very well with the decrease of the pH value. Liquid products of higher process temperatures show a lower pH value (see **Figure 29**). Overall, however, the H_2S plays only a minor role compared to DMS.

However, a clear tendency in favor of the DMS is not visible based on the volume fraction. The maximum is at T_R = 300 °C. After that, however, it drops again.

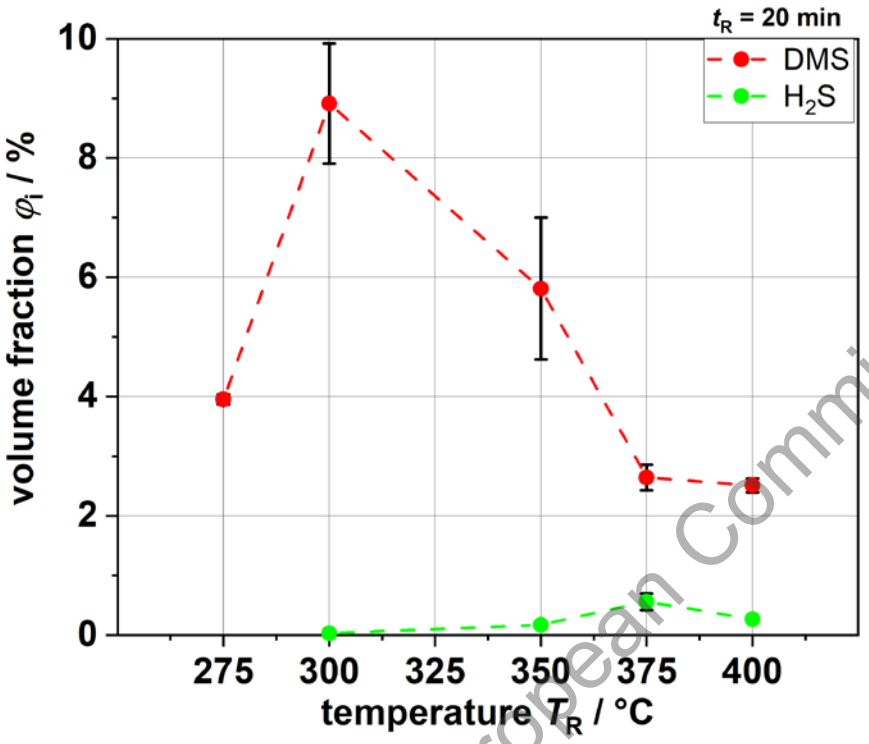

Figure 28: dimethyl sulfide (DMS) concentration and hydrogen sulfide (H_2S) volume fraction in the gas phase at different reaction temperatures T_R

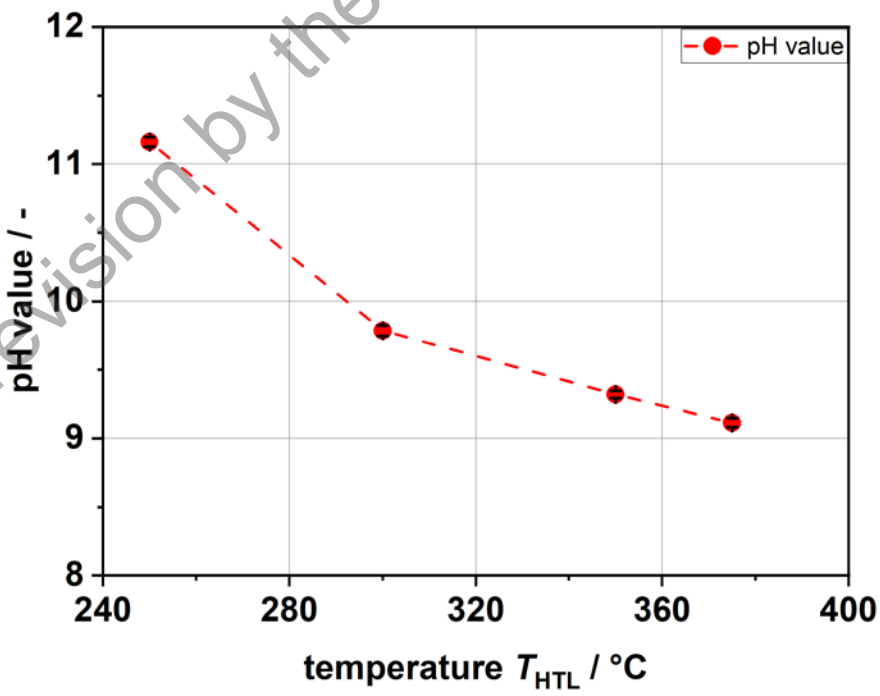

Figure 29: pH value for different liquid product phases at different reaction temperatures T_R

To get a more complete picture, we have plotted the sulfur content in the gas, which is related to the DMS, as a fraction of the total sulfur in the system (see **Figure 30**). Here, the mentioned problem with the different feedstock amounts is no longer present. The sulfur in the DMS accounts for between 5 wt. % to over 35 wt. % of the total sulfur in the feedstock. A clear increase towards T_R = 400 °C can be observed. This can partially explain the decrease in sulfur concentration in **Figure 19**. Although the points at T_R = 275 °C and T_R = 400 °C in both figures match, the progression is slightly different. Possible other sulfur components, e.g. acting as possible intermediates towards DMS, could be decisive for this. Due to the fact, that DMS is produced during the HTL process, we assume that there is a connection between the inorganic sulfur salts and the reaction to DMS. Therefore, we decided the already mentioned model liquors to investigate a possible connection between the sulfide ion concentration and the DMS production.

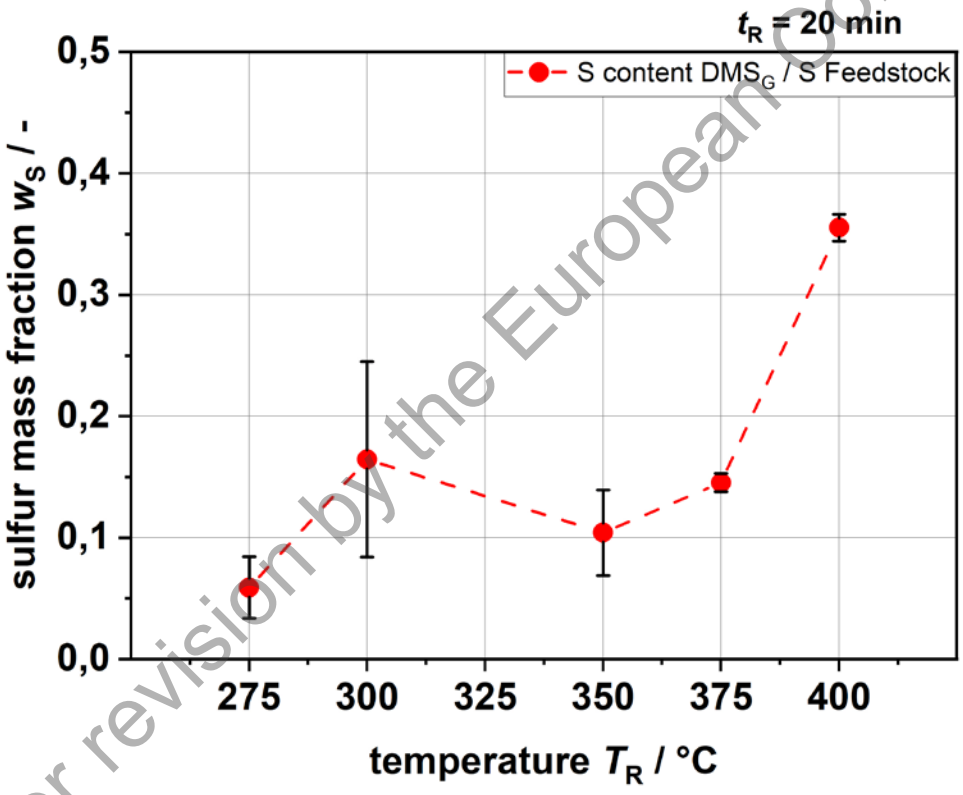

Figure 30: sulfur content of DMS in gas phase related to total sulfur in feedstock

3.2.2 Comparison between real and model black liquor

Before we started to work with the model BL, we had to confirm that the HTL of the model BL and the real BL deliver comparable results. **Figure 31** shows the normalized GC-MS chromatograms of both at a reaction temperature T_R = 375 °C and a holding time of t_R = 10 min. It is easily visible that the major peaks are at the same retention time. This is in good agreement for our produced model BL. With this result, it is possible to say that we can

compare the results of both experimental studies and can also transfer the information which we can get from the HTL of the model BL to the studies with the real BL. The major difference between both chromatograms are the height of the peaks. A possible explanation for this could be the difference in the organic matter since we have a lot more Lignin in our model BL. This issue also affected smaller peaks from compounds like acids or alcohols. They are not produced in visible amounts in the model BL that leads to a cleaner chromatogram. This is helpful especially for quantifying compounds, because there are no that much underlying peaks. One example for this is marked peak, catechol, in the black box. The red peak looks wider and less smooth than the green one. The reason for this is an acid, which has retention time very close to catechol and therefore has an effect on the peak shape.

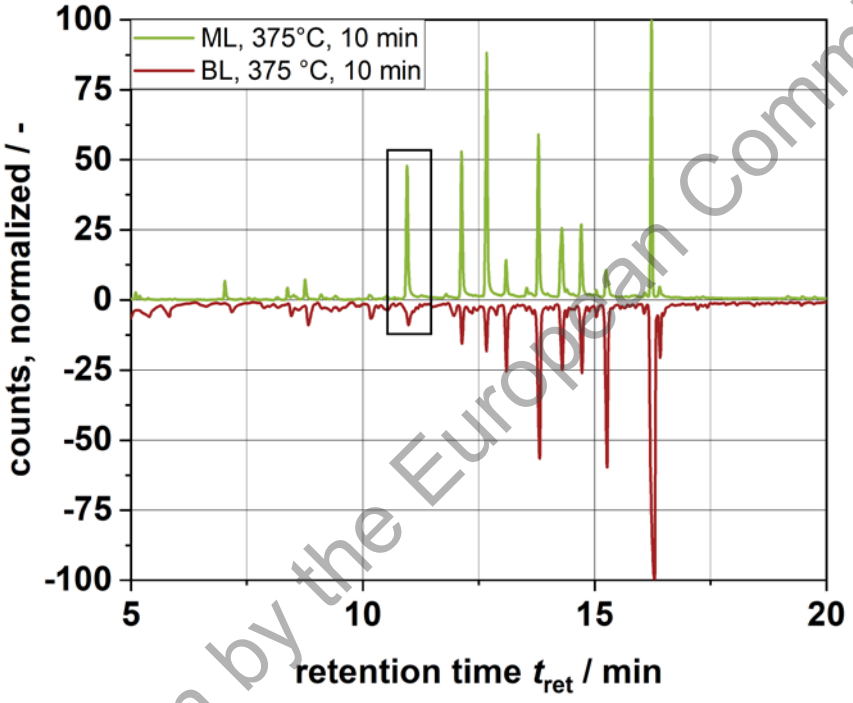

Figure 31: Comparison of GC-MS chromatograms of model BL (green, 3 g*l^{-1} HS$^-$) and real BL (red) at T_R = 375 °C and t_R = 10 min; highlighted peak in black box: Catechol

3.2.3 Influence of sulfide concentration on the HTL process

In order to investigate the relationship between the inorganic sulfur-containing salts and the formation of DMS during the HTL process, we used the prepared model liquors for the batch experiments. This was done using sulfide as an example. If the correlation is confirmed, an interaction of the inorganic salts with the organic mass is proven. Then other organic sulfur compounds could also be formed, which have not yet been detected. This is important information for the design of different upgrading processes. To adjust the different HS$^-$ concentrations, we added different amounts of sodium sulfide (Na_2S) to the model liquor. At the same time, a literature search was conducted to find a possible link between the HS- ion and DMS. In the process, the work of Karnofski et. al [14] was found. This work deals with the formation of odor during the Kraft process. The various organic sulfur compounds such as the

DMS are responsible for the odor generation. The paper also presents a possible reaction pathway leading to the formation of DMS. Here, the HS^- ion reacts with a methoxy group of the lignin structure. Especially in the case of hardwood, a large number of methoxy groups are present due to the structure of the sinapyl alcohol. As an intermediate, a methyl mercaptan is formed, which again donates a proton in the alkaline environment. The resulting ion reacts with another methoxy group and splits off as dimethyl sulfide.

$$HS^- + Lig - OCH_3 \rightarrow CH_3SH + Lig - O^-$$
$$CH_3SH + OH^- \leftrightarrow CH_3S^- + H_2O$$
$$CH_3S^- + Lig - OCH_3 \rightarrow H_3CSCH_3 + Lig - O^-$$

This reaction path can be very easily applied to this work. On the one hand, the force process is carried out under pressure and elevated temperatures in an aqueous environment, although under milder conditions, and on the other hand, both HS- ions and methoxy groups are present.

3.2.3.1 Gas phase

Figure 32 shows the volume fractions of DMS and H_2S at different HS^- concentrations. In addition, the volume fraction of another model liquid containing only sodium hydroxide (NaOH) and potassium hydroxide (KOH) is plotted in pink. This serves as a reference to the other model caustic solutions. Clearly visible is the increase of DMS with increasing HS^- concentration in the feedstock. This is a clear indication that the inorganic sulfides react with the lignin to form organic sulfur compounds. Furthermore, it confirms the first step of the reaction path of Karnofski et. al. The amount of H_2S also increases, but the amount is much lower compared to the DMS. At a HS^- concentration of 0 g/L, no H_2S could be detected. Presumably, the H_2S formation is mainly due to the equilibrium shift as written before. Interestingly, DMS is formed even without any sulfur-containing salts in the model solution, but less than with the model liquor with 0 g/L HS^- concentration. This may be due to several reasons. It could be that the lignin was still somewhat contaminated with salts. However, it is more likely that the sulfur present (see **Table 8**), which has been incorporated into the lignin structure by the Kraft process, forms the DMS.

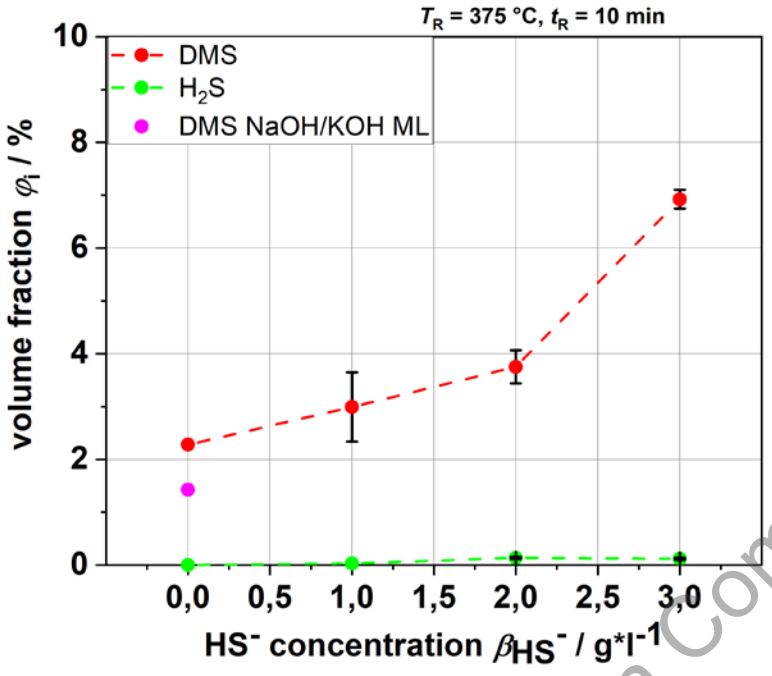

Figure 32: volume fraction of DMS and with different HS- concentration in feed; control feedstock (pink) without sulfur-containing salts (only NaOH/KOH+Lignin)

3.2.3.2 Monomer product yields

In addition to the formation of organic sulfur compounds such as DMS in connection with the HS^- concentration, it is also important to what extent the depolymerization of the lignin is influenced. For this purpose, we performed the same analyses as for the liquid product phase based on the real black liquor. **Figure 33** shows the yields of the typical aromatic monomers formed during depolymerization for different HS^- concentrations in the feedstock. A slight decrease of all quantified compounds can be observed. The largest decrease occurs with the first increase of HS^- ions in the feedstock. After that, the concentration remains stable within the error. It can be stated that the influence on the yields in the concentration range investigated is negative, but cannot be compared with the influence of temperature, which is clearly more visible.

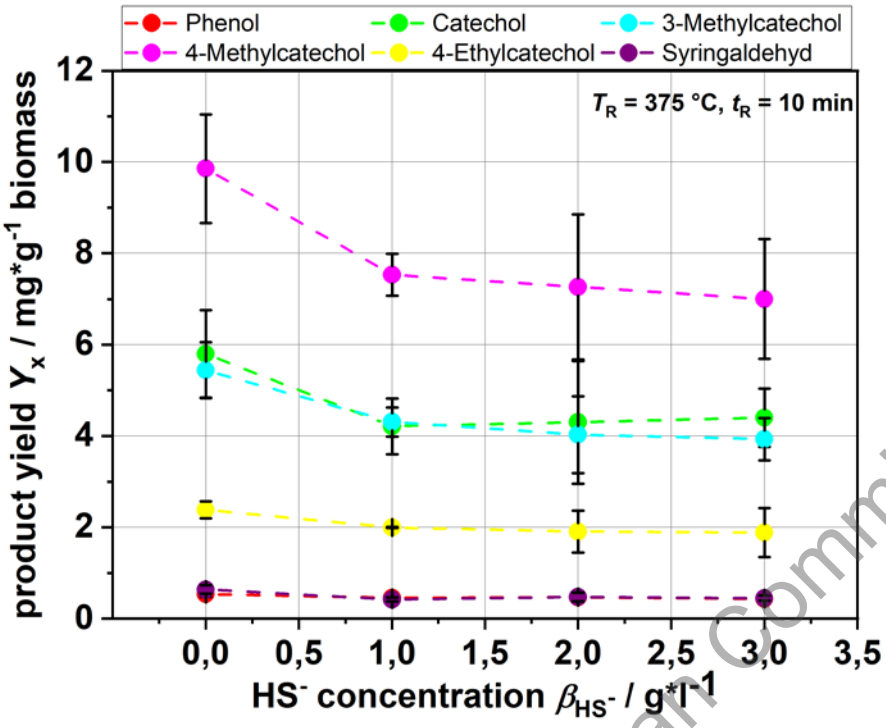

Figure 33: product yields of typical aromatic monomer compounds produced during HTL with model liquors with different HS- concentrations.

3.2.3.3 Biocrude yield & molecular weight

To analyze the depolymerization progress, the biocrude was first obtained again by extraction from the liquid product phase. The yields can be found in **Figure 34**. These are again very low. Whether the HS concentration has an influence on the yield is difficult to say with these amounts produced. Presumably, if there is an influence, it is rather small. **Figure 35** shows the molecular weight of the different biocrudes. Across all points, there is a trend towards lower molecular weight. Again, the lowest point is around 4000 g/mol. Together with the trend of yields of different monomers, this could indicate that the HS- concentration somewhat accelerates the depolymerization. The same correlation between decreasing yields and decreasing molecular weight is observed as with increasing reaction temperature or holding time, albeit on a smaller scale. Further experiments and analysis need to be performed to confirm this assumption. The assumption is also supported by the SEC chromatograms (see **Figure 36**). Except for the curve for a HS concentration of 2 g/l, the characteristics also fit to an accelerated depolymerization reaction with increasing HS concentration in the feedstock. Also the possible monomer peak at a retention time of about 10 min, which is outside the calibration limit, is highest at the highest concentration. Overall, it would make sense, if a higher HS- concentration accelerates the depolymerization of lignin. It is also used to separate the lignin from the cellulose fibers in the Kraft process. There, the sulfide is also breaking down some of the lignin structures and helps to form soluble compounds.

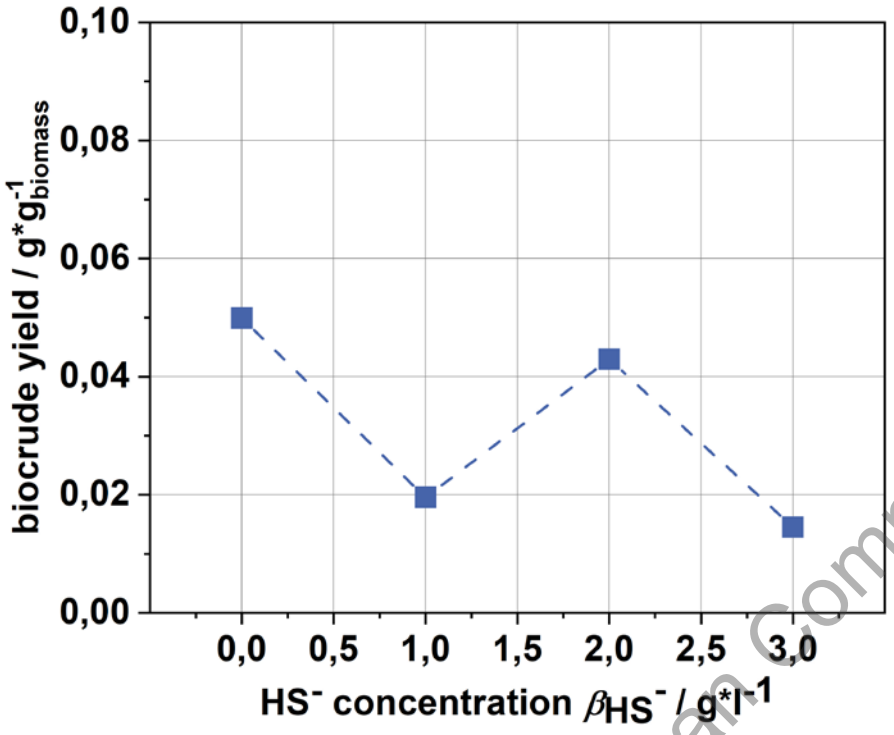

Figure 34: biocrude yields of HTL with model liquors with different HS- concentrations

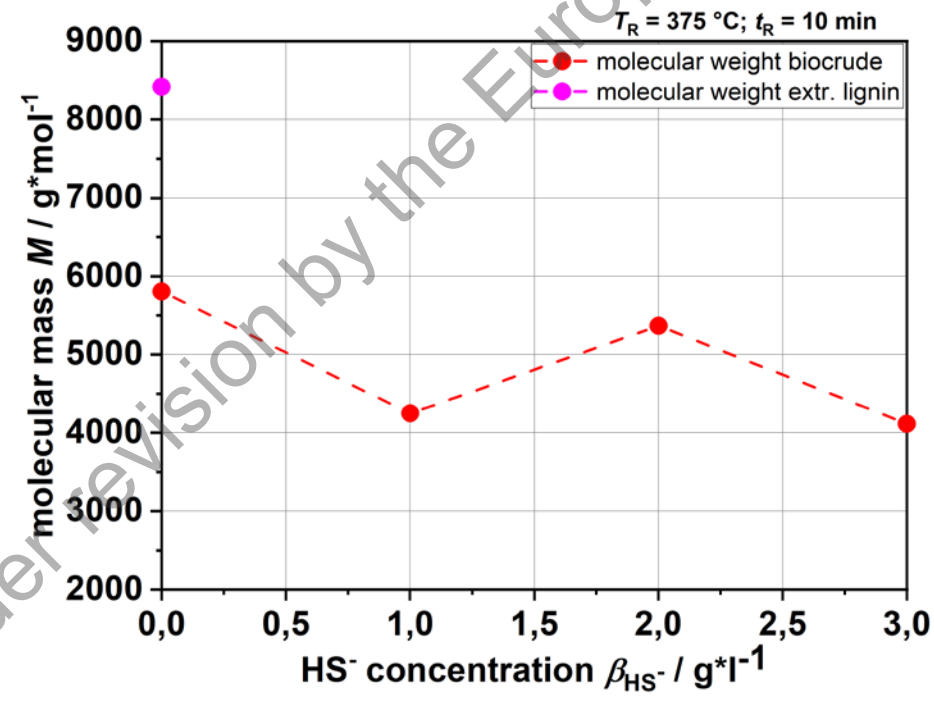

Figure 35: molecular weight of biocrude produced via HTL of model liquors with different HS- concentration

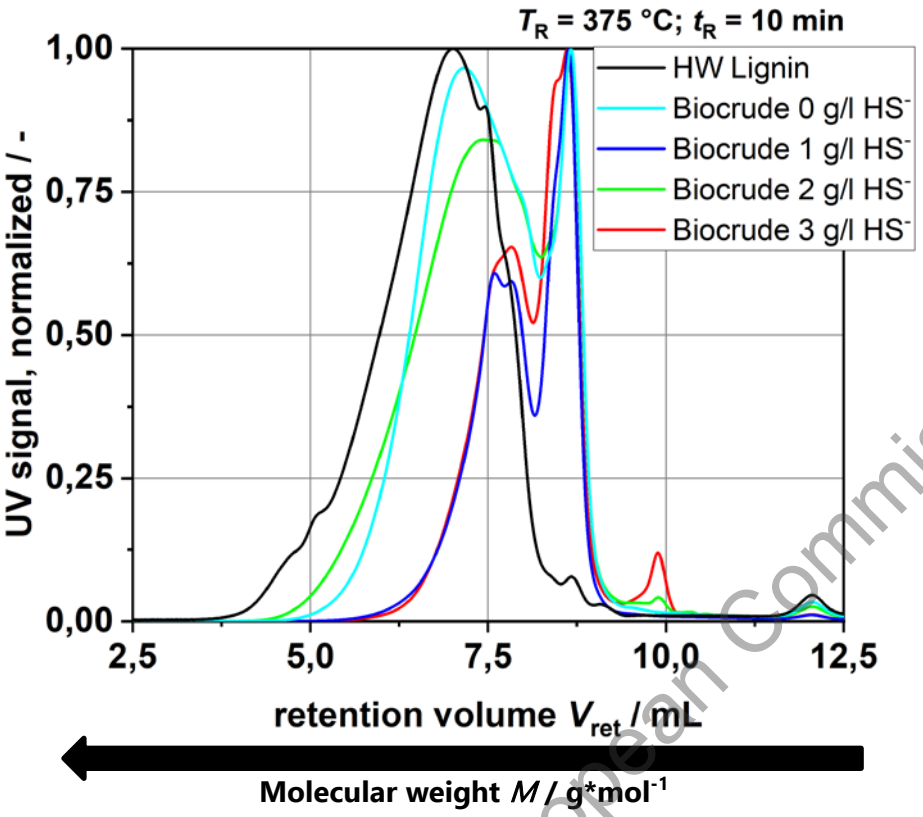

Figure 36: SEC chromatograms of biocrudes from model liquors with different HS- concentration; molecular weight decreasing with higher retention volume

4 Summary

In task 1.2, the HTL batch experiments of the black liquor from the pulp mill as well as with self-produced model liquors were carried out. For this purpose, micro autoclaves were used as reactors. In addition to the HTL process, the analysis of the different product phases obtained was also carried out. The different phases were separated, analyzed with different analytical methods, the application of which was possible within the scope of the project, and then the data obtained were analyzed and evaluated. We were able to establish a carbon mass balance, in which we were able to determine over 90 wt. % of carbon. However, the overall organic carbon in the liquid phase turned out to be decreasing at higher temperatures. . This also had an impact on the biocrude yields, which turned out to be very low. The results for HTL of lignin or BL in literature often shows higher yields [1]. Our experiments show that small holding times favor a higher output of organic carbon in the liquid phase, which helps also to get higher monomer yields and higher biocrude yields. We assume on the one hand, that cross-linking reactions of aromatics increase the carbon in the solid phase. On the other hand the batch design could be also a reason for it., This results need a comparison with the continuous experiments, which are part of the other tasks in WP1 and WP2. Regarding the process parameters for the continuous plant, the reaction temperature T_R should be not higher than 375 °C. The residence time should be also low, if it is possible under 10 minutes. The analysis of the extracted phase showed that catechol and its derivates are the main monoaromatic compounds. All the Catechols together lead to yields of around 1 – 2 % of the biomass in the feedstock. The highest yields are obtained at 300 °C. We were able to see, that aromatics with methoxy groups like syringol and guaiacol are intermediates. With higher temperature and holding time, hydroxyl and methyl groups are the main additions to the aromatic ring. Furthermore, a first simple reaction pathway could be established based on the data. The depolymerization process was visualized using SEC analysis and the molecular weight of the non-volatile organic fraction determined thereby. Interestingly, there appears to be a lower barrier at 4000 g/mol that could not be overcome in these experiments. Concerning the investigations on sulfur and its behavior during the process, we have looked in which product phases the sulfur ends up. The inorganic sulfur decreased, which is a first indication of the participation of the sulfur-containing salts in the reactions. Since the organic sulfur concentration in the liquid phase also decreased, we focused on the gas phase. We succeeded in identifying dimethyl sulfide as the main sulfur component. The sulfur content due to DMS in the gas phase alone was 10 – 20 % of the sulfur in feedstock at lower temperatures and over 35 % at 400 °C. Together with the DMS in the liquid phase, it is safe to say, that DMS is the main organo-sulfur compound produced during the HTL process. To prove that the inorganic salts, first of all the sulfide, react with the organic components of the lignin to form organic sulfur compounds like the DMS, we prepared the model liquors. These are based on feedstock characterization to get as close as possible to the real black liquor. The HS^- concentration was varied to observe its influence on the HTL process. The results show a clear correlation between the formation of DMS and the initial HS^- concentration. The first part of the reaction path found in the literature by Karnofski et. al [14] could thus also be confirmed. This leads to the

assumption that other organic sulfur compounds are also formed in the course of reactions between sulfur-containing salts and the lignin. Otherwise, a higher HS^- concentration seems to lead to a faster depolymerization. A decrease in molecular weight as well as reduced yields of the monomers indicate this.

5 Outlook

This work is considered the basis for the development of a reaction kinetic model, which will be developed in the near future. For this purpose, further analyses will be carried out, such as NMR analyses of the biocrude. An idea to improve the biocrude yields is the extraction of organic compounds from the solid product phase with acetone. It is possible, that organic molecules are bound to the solid surface. The extracted compounds will be also analyzed via EA, ICP and NMR. At the moment, experiments with model substances such as guaiacol and syringol are taking place. The results of these, together with the results of this work, should provide an even clearer picture of the formation of various product substances. In addition, the possible differences to the softwood black liquor will be investigated. The results should help to better design the continuous process to achieve desired results. The study of sulfur behavior will serve to better address potential difficulties in the implementation of upgrading or reforming processes, which are also being worked on as part of the BL2F project. The knowledge gained can help to optimally design catalysts, process parameters or even construction materials. In conclusion, the batch experiments provide a good basis for further research on this topic. Regarding the other WP especially concerning with the continuous experiments the optimal reactions conditions for the batch experiments could be a good starting point for their process.

6 References

1. Lappalainen J, Baudouin D, Hornung U et al. (2020) Sub- and Supercritical Water Liquefaction of Kraft Lignin and Black Liquor Derived Lignin. Energies 13:3309. https://doi.org/10.3390/en13133309
2. Akhtar J, Amin NAS (2011) A review on process conditions for optimum bio-oil yield in hydrothermal liquefaction of biomass. Renewable and Sustainable Energy Reviews 15:1615–1624. https://doi.org/10.1016/j.rser.2010.11.054
3. Forchheim D, Hornung U, Kempe P et al. (2012) Influence of RANEY Nickel on the Formation of Intermediates in the Degradation of Lignin. International Journal of Chemical Engineering 2012:1–8. https://doi.org/10.1155/2012/589749
4. Dastpak A, Lourençon TV, Balakshin M et al. (2020) Solubility study of lignin in industrial organic solvents and investigation of electrochemical properties of spray-coated solutions. Industrial Crops and Products 148:112310. https://doi.org/10.1016/j.indcrop.2020.112310
5. Wang C, Fan Y, Hornung U et al. (2020) Char and tar formation during hydrothermal treatment of sewage sludge in subcritical and supercritical water: Effect of organic matter composition and experiments with model compounds. Journal of Cleaner Production 242:118586. https://doi.org/10.1016/j.jclepro.2019.118586
6. Forchheim D, Hornung U, Kruse A et al. (2014) Kinetic Modelling of Hydrothermal Lignin Depolymerisation. Waste Biomass Valor 5:985–994. https://doi.org/10.1007/s12649-014-9307-6
7. Arturi KR, Strandgaard M, Nielsen RP et al. (2017) Hydrothermal liquefaction of lignin in near-critical water in a new batch reactor: Influence of phenol and temperature. The Journal of Supercritical Fluids 123:28–39. https://doi.org/10.1016/j.supflu.2016.12.015
8. Schuler J, Hornung U, Dahmen N et al. (2019) Lignin from bark as a resource for aromatics production by hydrothermal liquefaction. GCB Bioenergy 11:218–229. https://doi.org/10.1111/gcbb.12562
9. Schuler J, Hornung U, Kruse A et al. (2017) Hydrothermal Liquefaction of Lignin. JBNB 08:96–108. https://doi.org/10.4236/jbnb.2017.81007
10. Belkheiri T, Andersson S-I, Mattsson C et al. (2018) Hydrothermal Liquefaction of Kraft Lignin in Subcritical Water: Influence of Phenol as Capping Agent. Energy Fuels 32:5923–5932. https://doi.org/10.1021/acs.energyfuels.8b00068
11. Orebom A, Verendel JJ, Samec JSM (2018) High Yields of Bio Oils from Hydrothermal Processing of Thin Black Liquor without the Use of Catalysts or Capping Agents. ACS Omega 3:6757–6763. https://doi.org/10.1021/acsomega.8b00854

12. Takenaka N, Furuya S, Sato K et al. (2003) Rapid reaction of sulfide with hydrogen peroxide and formation of different final products by freezing compared to those in solution. Int J Chem Kinet 35:198–205. https://doi.org/10.1002/kin.10118

13. Jeyakumar S, Rastogi RK, Chaudhuri NK et al. (2002) DETERMINATION OF SULPHUR SPECIES IN THE PRESENCE OF COMMON ANIONS WITH INDIRECT MEASUREMENT OF SULPHIDE BY ION CHROMATOGRAPHY (IC). Analytical Letters 35:383–395. https://doi.org/10.1081/AL-120002537

14. Karnofski MA (1975) Odor generation in the kraft process. J Chem Educ 52:490. https://doi.org/10.1021/ed052p490